CAPITAL UNIVERSITY OF SCIENCE AND TECHNOLOGY, ISLAMABAD

Safety Evaluation and in-vivo Toxicity Assessment of Green-Synthesized Zinc Sulfide Nanoparticles with *Justicia adhatoda* Extract on Rat Model

by

Iqra Sajid

A thesis submitted in partial fulfillment for the degree of Master of Science

in the

Faculty of Health and Life Sciences
Department of Bioinformatics and Biosciences

2025

*I dedicate my work to my family, friends and to my teachers. Specially, with a feeling of gratitude I dedicate this work to my loving parents, my sisters (**Hira Sajid, Rameesha Sajid**) and my brother (**M. Romaan Sajid**) for their munificent support they provided me throughout my entire life. I thank them wholeheartedly of their unconditional love, prayers and support.*

CERTIFICATE OF APPROVAL

Safety Evaluation and in-vivo Toxicity Assessment of Green-Synthesized Zinc Sulfide Nanoparticles with *Justicia adhatoda* Extract on Rat Model

by

Iqra Sajid

(MBS233008)

THESIS EXAMINING COMMITTEE

S. No.	Examiner	Name	Organization
(a)	External Examiner	Dr. Sidra Rehman	COMSATS, Islamabad
(b)	Internal Examiner	Dr. Erum Dilshad	CUST, Islamabad
(c)	Supervisor	Dr. Sania Riaz	CUST, Islamabad

Dr. Sania Riaz
Thesis Supervisor
May, 2025

Dr. Syeda Marriam Bakhtiar
Head
Dept of Bioinformatics & Biosciences
May, 2025

Dr. Sahar Fazal
Dean
Faculty of Health & Life Sciences
May, 2025

Author's Declaration

I, **Iqra Sajid** hereby state that my MS thesis titled "**Safety Evaluation and in-vivo Toxicity Assessment of Green-Synthesized Zinc Sulfide Nanoparticles with *Justicia adhatoda* Extract on Rat Model**" is my own work and has not been submitted previously by me for taking any degree from Capital University of Science and Technology, Islamabad or anywhere else in the country/abroad.

At any time if my statement is found to be incorrect even after my graduation, the University has the right to withdraw my MS Degree.

(Iqra Sajid)

Registration No: MBS233008

Plagiarism Undertaking

I solemnly declare that research work presented in this thesis titled "**Safety Evaluation and in-vivo Toxicity Assessment of Green-Synthesized Zinc Sulfide Nanoparticles with *Justicia adhatoda* Extract on Rat Model**" is solely my research work with no significant contribution from any other person. Small contribution/help wherever taken has been duly acknowledged and that complete thesis has been written by me.

I understand the zero tolerance policy of the HEC and Capital University of Science and Technology towards plagiarism. Therefore, I as an author of the above titled thesis declare that no portion of my thesis has been plagiarized and any material used as reference is properly referred/cited.

I undertake that if I am found guilty of any formal plagiarism in the above titled thesis even after award of MS Degree, the University reserves the right to withdraw/revoke my MS degree and that HEC and the University have the right to publish my name on the HEC/University website on which names of students are placed who submitted plagiarized work.

(Iqra Sajid)

Registration No: MBS233008

Acknowledgement

In the name of **Allah**, the most gracious and the most merciful; and prayers and **peace be upon Muhammad**, His servant and messenger. I would like to acknowledge my limitless thanks to Allah Almighty and to his last **Prophet Muhammad (S.A.W)** without their guidance this work would have never become completed. I owe a deep depth of gratitude to our **University, Capital University of Science & Technology (CUST)** for giving me such an opportunity to complete this work. A special thanks to the Dean & Head of the Department of Bioinformatics and Biosciences **Dr. Sahar Fazal** & **Dr. S. Marriam Bakhtiar** for encouraging and the most of all patience throughout the entire process.

I would like to acknowledge the instrumental advice and support of my Supervisor **Dr. Sania Riaz** who has been very generous in the conduction and writing of this thesis. I thank her from the bottom of my heart. A special thanks to all others who helped me during my research especially. I would like a warm thanks to my beloved friends, **Nauman Khalid, Dr. Mariam Tariq, Nouman Shahzad Malik** and **Sadia Malik** who have been supportive along the way of doing my research work.

I want to express my wholehearted thanks to my family who have provided me support throughout in doing my research. Their constant support, encouragement and willingness to help at every step is truly remarkable.

(Iqra Sajid)

Abstract

Nanoparticles can cause nanotoxicity through a number of pathways that relate to their specific physical and chemical properties. The toxicity of Green -Synthesized ZnS NPs is also significantly influenced by their surface characteristics. Long-term systemic exposure to green synthesized ZnS NPs can cause serious homeostasis disruptions, which may have a negative impact on hematological parameters and general health. The *Justicia adhatoda* plant extract was used to synthesize Zinc sulfide nanoparticles. The NPs were subjected to detailed characterization including SEM, FTIR, EDX, XRD and UV-Visible Spectroscopy. After characterization the effect of low dose (1.73 mg/200g) and high dose (3.46mg/200g) Green –Synthesized ZnS NPs was checked on Sprague-Dawley rat model for 20 days. The in-vivo toxicity and safety profile assessment was checked using morphological, biochemical, histopathological and hematological response of rats after intake of Green-synthesized ZnS NPs. The results showed significant differences in different parameters like RBC Count, WBC Count, platelets, ALT, AST, Urea and creatinine level by making a comparison with control group through statistical analysis (one-way ANOVA). According to histopathological response low dose group shows mild cytoplasmic vacuolation within hepatocytes and mild metabolic stress, possibly due to early-stage toxic or nutritional disturbances while high dose group shows mild portal inflammation with prominent vacuolar degeneration in hepatocytes and these changes are consistent with mild liver injury. So, a comprehensive research and updated data is necessary to assess Green- synthesized ZnS NPs safety profile, particularly with regard to their biocompatibility in biological systems and long-term exposure.

Contents

List of Figures

List of Tables

Abbreviations

ALP	Alkaline phosphatase
ALT	Alanine transaminase
AST	Aspartate aminotransferase
CT SCAN	Computed Tomography Scan
EDTA	Ethylenediaminetetraacetic acid
EDX	Energy dispersive X-ray
EOS	Eosinophils
FTIR	Fourier-transform infrared spectroscopy
Hb	Hemoglobin
IST	Institute of space and technology
LFT	Liver function test
LYMPHO	Lymphocytes
MCH	Mean corpuscular hemoglobin
MCHC	Mean corpuscular hemoglobin concentration
MCV	Mean corpuscular volume
MONO	Monocytes
MRI	Magnetic Resonance Imaging
NBF	Neutral-buffered formaldehyde
NEU	Neutrophils
PET SCAN	Positron Emission Tomography
PLT	Platelets
RBC	Red blood cells
RFT	Renal function test
ROS	Reactive oxygen Species

SEM	Scanning electron microscopy
UV-Vis spectroscopy	Ultraviolet -Visible Spectroscopy
WBC	White blood cells
XRD	X-ray diffraction
ZnS NPs	Zinc sulfide nanoparticles

Chapter 1

Introduction

Nanoparticles are typically classified as particles sized between 1 and 100 nanometers. They can also be classified according to shape, unique properties, or composition. Nowadays the widespread use of nanotechnology in various fields, especially environmental science and health scientists' fuels to make this subject matter one of the most interesting research areas that have attracted attention It has raised a lot of interest and contribution in their manufacture and their impacts on biological systems [1].

Zinc sulfide nanoparticles (ZnS NPs) are semiconductor-like nanoscale particles of zinc sulfide ranging in size from a few nanometers (1 to 100 nm), these particles have unique characteristics that make them apart from bulk ZnS because of their small size and large surface area [2]. Their microscopic properties make them unique and suitable in the development of modern medicine, immense chemical reactivity, bio mobility and energy absorption [2].

The surface chemistry of Zinc sulfide nanoparticles (ZnS) can be more precisely adjusted to accomplish particular functionalization, improving their efficacy in biocatalysis, environmental sensing, and targeted drug administration [3, 4]. They are useful in photocatalytic applications such as pollutant degradation because the green synthesis process may include functional groups that increase reactivity. By ensuring that the nanoparticles are generated with the least possible impact on

the environment, the green synthesis approach makes them more sustainable for large-scale applications [3].

Zinc sulfide nanoparticles (ZnS NPs) are effective fluorescent markers for bioimaging because of their high photoluminescence. They can be employed in optical imaging methods to provide high- resolution images of tissues, cells, or biological processes. ZnS NPs can be used as carriers for drug delivery, especially for targeted treatments [3].

Therapeutic substances can be released under controlled conditions by functionalizing their surface with biocompatible coatings or ligands that bind to particular cells. They are therefore perfect for treating cancer, since it is essential to precisely target tumor cells in order to minimize adverse effects [4].They are used in biosensors, where their surface changes enable them to identify specific biomolecules, infections, or poisons, producing visible responses such as fluorescent for environmental monitoring and diagnosis. They are appropriate for various biomedical applications due to their low toxicity and biocompatibility [5].

Nanoparticles can cause nanotoxicity through a number of pathways that relate to their specific physical and chemical properties. The nanotoxicity of ZnS NPs is also significantly influenced by their surface characteristics [6]. ZnS NPs that are uncoated or non- functionalized, for example, may have stronger surface reactivity, which in turn might lead to the unwanted interactions with cells. They have high reactivity due to their high surface area to volume ratio, which then can interfere with biological functions that subsequently trigger immunological responses [6, 7]. ZnS NPs can interact with numerous cellular components after internalization, causing oxidative stress and cytotoxicity. Reactive oxygen species (ROS) generated by the ZnS NPs results in oxidative stress that disrupts lipids, proteins, and DNA in cells with possibilities such as apoptosis or inflammation or genotoxicity [6].

Understanding nanotoxicity is essential to grasping long-term effects, especially for consumers purchasing products containing nanoparticles and workers in organizations using nanomaterials [8]. To ensure safety, compliance, and the responsible

development of nanotechnology, it is crucial to comprehend nanotoxicity. It is essential for safeguarding both the environment and human health while facilitating the development of novel materials and applications [7, 8].

According to in vivo studies, ZnS NP exposure can cause an inflammatory response. This could release of pro-inflammatory cytokines and the activation of immune cells like macrophages. Chronic inflammation can lead to long-term health implications and tissue damage [8].

Moreover, ZnS NPs can build up in organs such as the kidneys, liver, and lungs, where they are difficult to remove or metabolize. This might result in bioaccumulation and long-term exposure hazards [7].This is especially problematic for ZnS NPs used in biomedical applications because repeated exposure can raise the risk of long-term consequences such organ damage and inflammation.

Biologically synthesized ZnS nanoparticles (ZnS NPs) which are made utilizing biological agents or plant extracts, possesses several unique properties due to the eco-friendly and biocompatible methods used in their synthesis. Their homogeneous distribution and generally smaller size result in increased surface area [9]. Using plant extracts, green synthesis provides a sustainable and environmentally friendly method of synthesizing nanoparticles.

When compared to their chemically manufactured counterparts, these NPs frequently exhibit better biocompatibility, which makes them more applicable for use in both biological and medical applications.

The Green synthesis of ZnS Nanoparticles with *Justicia adhatoda* plant extract lead to the stabilization and reduction of ZnS NPs, the application of *Justicia adhatoda* extract provides additional therapeutic advantages associated to the phytochemicals in the plant. *Justicia adhatoda* commonly known as Malabar nut or vasaka. [5] It belongs to the family Acanthaceae.

The comprehensive assessment of in-vivo toxicity of ZnS NPs using extract from *Justicia adhatoda* will bring knowledge on their biocompatibility and explain their any potential toxicity processes. In order to ensure the safety of possible medical

interventions and evaluate the possibility of utilizing green-synthesized ZnS NPs in biomedical applications, this work is crucial. [10].

1.1 Problem Statement

Long-term systemic exposure to green synthesized ZnS NPs can cause serious homeostasis disruptions, which may have a negative impact on hematological parameters and general health. Increased inflammation and oxidative stress in many organs can hinder organ function and raise long-term health risks. Comprehensive research is necessary to assess these nanoparticles safety profile, particularly with regard to their biocompatibility in biological systems and long-term exposure

1.2 Hypothesis

Green synthesized ZnS NPs using plant *Justicia adhatoda* may have biochemical, hematological and histopathological toxicity.

1.3 Gap Analysis

There were various studies that examined the toxicity of Green-synthesized ZnS nanoparticles that come in contact with biological systems thus trigger the oxidative stress in the biological system and generate reactive oxygen species (ROS). But there are a lack of information about the interaction of Green-synthesized ZnS NPs using *Justicia adhatoda* plant extract within complex biological systems which is a significant gap in our knowledge. Key unknowns include their biodistribution, accumulation in specific organs, long-term toxicity, and potential immunogenicity when administered in vivo. Filling this gap is essential for establishing the safety profile of *Justicia adhatoda*-synthesized ZnS NPs for biomedical and environmental applications. A well-designed clinical trial help in investigating the in-vivo toxicity of Green- synthesized ZnS nanoparticles.

1.4 Aim and Objectives

The aim of the study is to check the safety profile of Green-synthesized ZnS nanoparticles. It will be aligned by following objectives:

- To synthesize and characterize Green synthesized ZnS NPs
- To evaluate the in-vivo toxicity and safety profile of Green-synthesized ZnS NPs using biochemical, histopathological and hematological response of rats after intake of Green-synthesized ZnS NPs nanoparticles

Chapter 2

Literature Review

2.1 Nanomedicines and Nanotechnology

Materials with improved qualities, much greater strength, reduced weight, and improved chemical resistance, can be synthesized by the applications of nanotechnology. Nanoparticles, which range in size from 1 to 100 nanometers, are used in nanomedicine, a use of nanotechnology in healthcare, to interact with biological molecules both inside and on the surface of cells. With the help of nanoparticles, medicines and drugs can be delivered directly to certain cells, such as cancer cells, reducing side effects and enhancing efficacy [11].

Drug delivery is one of the main uses of nanomedicine. [12, 13]. Therapeutic substances can be encapsulated in nanoparticles, enabling precise and controlled drug delivery. This increases a drug's bioavailability, reduces adverse effects, and boosts therapeutic effectiveness. Nanomaterials improve resolution in imaging by acting as contrast agents in MRI, CT, and PET scans. Using nanoparticles for treatments including gene therapy, photothermal therapy, and vaccine delivery is another aspect of nanomedicine. [11].

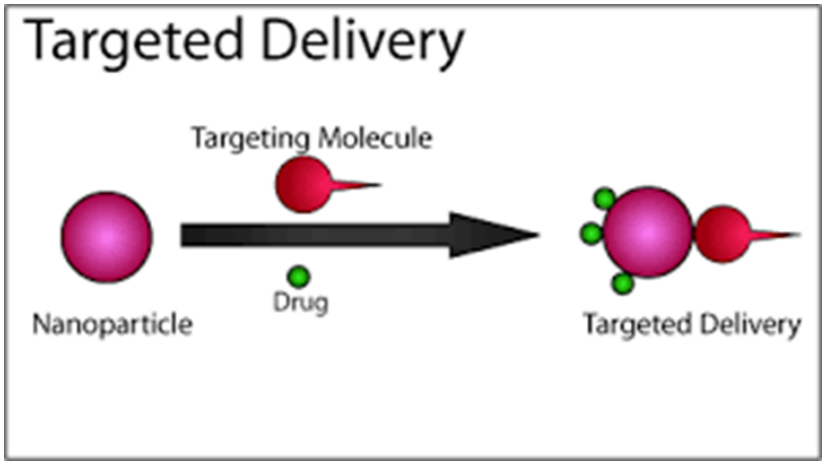

FIGURE 2.1: Nanoparticle-Based Drug Delivery [1]

Applications of nanomedicine include developing nanomaterials for real-time glucose monitoring in the management of diabetes, employing targeted nanoparticles in chemotherapy to improve cancer treatments by minimizing damage to healthy cells [13].

2.2 Properties of Nanoparticles

Nanoparticles have high surface area-to-volume ratio, which increase their reactivity and interaction with other materials. Nanoparticles can exhibit size-dependent optical, electrical, and chemical properties. A wide range of materials can be used to make them including metals, semiconductors, and polymers [14, 15]. They are helpful in delivering drugs and diagnostics because of their small size across biological barriers.

2.2.1 Functionalization and Targeting of Nanoparticles

Specific environments or applications can be targeted by the surface of nanoparticles that are functionalized with different chemicals. Sensors and imaging technologies further enhance the optoelectronics because they can modulate the light

absorption and scattering. They show highly influenced behaviour by the features like size, shape, and surface charge which can be managed by the synthesis techniques [16, 17].

2.2.2 Drug Delivery Applications

Nanoparticles can enhance the targeting, effectiveness, and bioavailability of medicinal drugs, as a result, nanoparticles are commonly used in drug delivery systems [16]. By binding ligands or antibodies to their surface, they can be designed to deliver medications directly to particular cells or tissues, including cancer cells, enabling targeted drug delivery [18]. This enhances the therapeutic effect while reducing adverse effects on healthy cells.

2.2.3 Controlled Drug Release and Enhanced Bioavailability

Nanoparticles allow for a slow and controlled release of the drugs, which in turn, decreases the frequency of doses and improves patient compliance [19]. They are also capable of turning poorly water-soluble medications into more soluble ones which then lead to better absorption and bioavailability. Their ability to cross biological barriers is another notable application. Nanoparticles can be modified with ligands, polymers, or a number of other compounds. These changes make it easier for nanoparticles to bypass the immune system and more efficiently reach their intended cells

2.2.4 Stimuli-Responsive Drug Release

Different nanoparticles can be designed to release a controlled payload such as drug, which is based on the certain triggers such as the variation in temperature, pH, or enzyme concentrations [20]. This regulated release enhances the therapeutic efficacy and reduce the adverse consequences.

2.2.5 Environmental Applications

The high reactivity of nanoparticles is one of the main reasons for their use in environmental applications. For example, Iron nanoparticles are used in specific water treatment processes to destroy chlorinated organic compounds and chlorinated plastics which can then be converted to less hazardous forms [21]. The nanoparticles' reactivity is responsible for the development of very efficient coatings and air filters in different applications that either absorb the pollutants eliminate pollutants in commercial or residential environments.

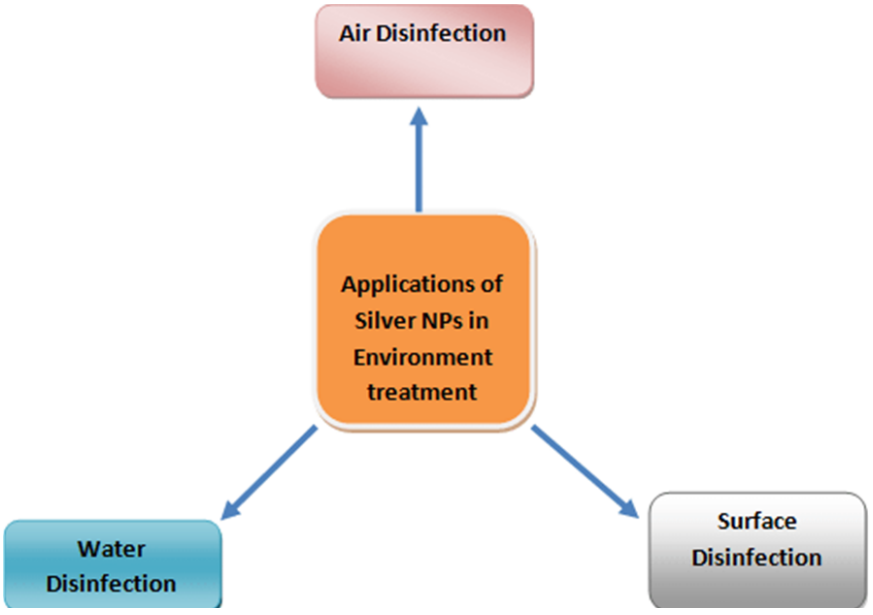

FIGURE 2.2: Applications of silver nanoparticles in environment treatment [22]

2.2.6 Medical Applications and Biological Barrier Penetration

Due to their smaller size as compared to larger particles, nanoparticles can easily cross the various types of biological barriers and target the tissues they are supposed to cure in case of medicine. Lipid nanoparticles, for instance, have been have played a crucial role in the administration of mRNA vaccine administration due to their ability to both transport and keep mRNA molecules inside the cells [23]. Drugs are also delivered through dendrimers and polymeric nanoparticles

that, in turn, provide the possibility of the controlled release and reduce side effects. Thus, the lower complexity of nanoparticles transforms them into the most optimal class of carrier for drug delivery [23].

2.2.7 Safety Concerns and Toxicity

Despite these benefits, worries over the possible toxicity and environmental effects of nanoparticles are raised by their small size and strong reactivity. Certain nanoparticles may interact with biological tissues in unexpected ways when inhaled, consumed, or absorbed, which could have negative consequences. Therefore, a crucial area of continuing research to guarantee the safe use of these materials is the study of nanoparticle toxicity, bioaccumulation, and environmental persistence [24].

2.3 Approaches for the Synthesis of Nanoparticles

There are two main approaches for synthesizing nanoparticles: top-down and bottom-up approach.

2.3.1 Top-down Approach

In "top-down" approach, the large pieces of material are broken down to generate the required nanostructure. Although top-down approaches are scalable and rather easy to use, they may result in particles with flaws and less control over their size and shape [25]. Ball milling is a top-down approach to crush the particles at the nanoscale while lithography uses light or electron beams in order to create particles at nanoscale surface [26].

2.3.2 Bottom-up Approach

In bottom-up approach molecules self-assemble themselves and build up in order to create nanostructures or by creating nanoparticles atom by atom or molecule by molecule, typically through chemical or biological synthesis. Although they can be difficult to scale up reliably, bottom-up approaches typically offer greater control over the size, composition, and structure of nanoparticles and are frequently more environmentally and energy-efficient [27].

For example, Silver nanoparticles made biologically have stronger antibacterial properties and can be applied to medical products, coatings, and wound dressings. Plant extracts are used to create gold nanoparticles, which have been examined for medication delivery, imaging, and diagnostics because of their biocompatibility and simplicity of functionalization. Compared to their chemically created counterparts, biologically synthesized nanoparticles are less hazardous, environmentally friendly, and utilize renewable resources [28, 29].

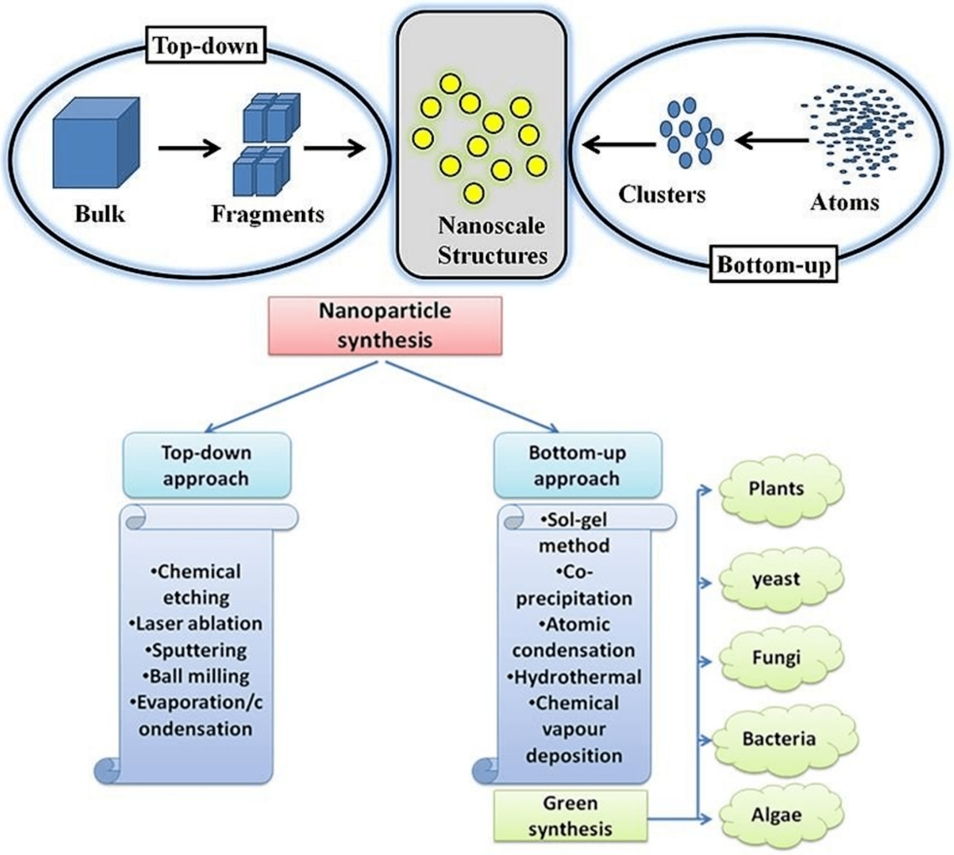

FIGURE 2.3: Top-down approach and bottom-up approach classifications [25, 26]

2.4 Method for Synthesis of Nanoparticles

There are following methods of synthesis of nanoparticles:

- Chemical methods by using sol-gel, hydrothermal, solvothermal, vapor synthesis [30]
- Biological methods using microbial and plant extract
- Physical or mechanical methods using milling, mechanical alloying

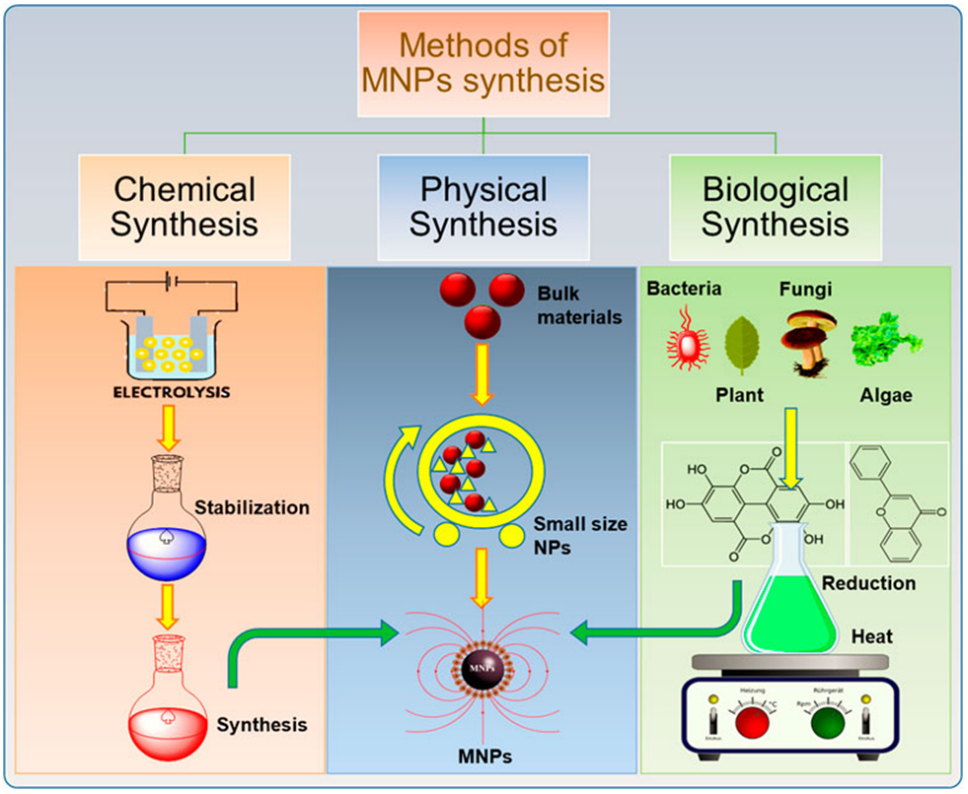

FIGURE 2.4: Methods of Synthesis of Nanoparticles [30]

2.5 Nanotoxicology

Nanotoxicity is important for a number of reasons. Knowing the possible health and environmental effects of nanoparticles is crucial as their use spreads throughout many industries. Unexpected harmful consequences that conventional materials might not show can result from the special qualities of nanomaterials, such as enhanced reactivity and changed biological interactions [31].

Nanoparticles have the ability to activate immune responses, leading to immunological suppression or inflammation, which can harm tissue or raise the risk of autoimmune reactions. Because certain nanoparticles can interfere with cellular processes or interfere with normal cell division, they may cause DNA damage or mutations, increasing the risk of cancer. Skin penetration by nanoparticles used in sunscreens and cosmetics can cause sensitization, allergic responses, or irritation in sensitive people. In addition, work indicates that some nanoparticles may be able to pass through the placental barrier and affect fetal development; studies on animals also indicate possible connections between exposure to nanoparticles and developmental defects, decreased fertility, or reproductive damage [32].

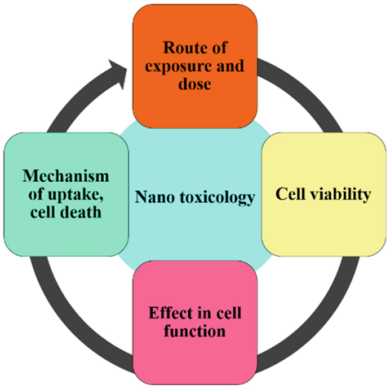

FIGURE 2.5: Toxicity Assessment of Nanoparticle [33]

2.6 Types of Nanoparticles

Classification of Nanoparticles according to their size, morphology, physical, and chemical properties often determines their function [34].

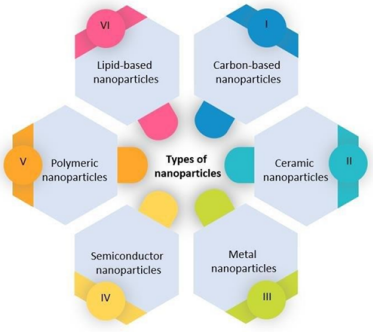

FIGURE 2.6: Different types of Nanoparticles [35]

2.6.1 Carbon-Based Nanoparticles

There are several types of carbon-based nanoparticles, each with special qualities and uses. Because of their exceptional strength, electrical conductivity, and thermal characteristics, carbon nanotubes are cylindrical structures that find application in drug delivery, electronics, and materials research [36]. Because of its exceptional electrical conductivity, mechanical strength, and vast surface area, graphene oxide organized in a two-dimensional lattice is well-suited for use in energy storage, sensors, and the biomedical industry. Because of their special qualities, fullerenes spherical molecules made completely of carbon can be utilized as antioxidants and in drug administration. Carbon dots are tiny carbon nanoparticles that are employed as sensors and in bioimaging because they glow when exposed to light [37]. Because of their unique qualities, these carbon-based nanoparticles are being investigated more and more for a range of uses, which makes them crucial for the advancement of both technology and medicine.

2.6.2 Ceramic Nanoparticles

Inorganic nanoparticles made of metal oxides, carbides, nitrides, or silicates are known as ceramic nanoparticles. Ceramic nanoparticles are becoming more and more popular in industries including biomedicine, electronics, and environmental remediation because of their exceptional mechanical strength, chemical stability, and resistance to heat [38, 39]. They have proven to be an effective medicine delivery mechanism for a number of illnesses, including cancer, glaucoma, and bacterial infections [40].

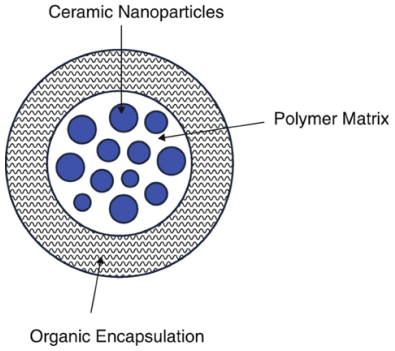

FIGURE 2.7: Schematic representation of ceramic nanoparticles [35]

2.6.3 Metallic Nanoparticles

Metals form metallic nanoparticles, which are tiny particles usually within the range of 1 to 100 nanometers. Because of their small size and vast surface area in relation to volume, hence the physical, chemical behavior, and reactivity of the nanoparticles are different from their bulk counterparts. [41] Gold nanoparticles are known for their biocompatibility in a variety of biomedical domains, including medication administration, imaging, and photothermal therapy, which uses heat generated from light to kill cancer cells [42].

2.6.4 Semiconductor Nanoparticles

One kind of nanoparticle that has characteristics with metals and non-metals is a semiconductor nanoparticle. Zinc sulfide (ZnS) nanoparticles, in particular, are semiconductor nanoparticles that scientists mainly investigate due to their excellent optical and electric properties [43]. ZnS nanoparticles predominantly have a size of 1 nm – 100 nm and contain crystalline arrangements of zinc and sulfur atoms. Their small size cause them to display quantum confinement phenomena, which results in size-dependent optical characteristics including photoluminescence and a bandgap that may be adjusted. High stability, low toxicity, and the ability to generate visible light when excited by UV radiation are some of the excellent properties of ZnS nanoparticles [44]. Semiconductor nanoparticles are used in biomedical applications for imaging, and diagnostics due to their brilliant fluorescence and capacity to target particular cells or tissues.

2.6.5 Polymeric Nanoparticles

The use of polymers to generate polymeric nanoparticles gives them great versatility for use in biomedical applications like gene therapy, medication administration, and medical imaging. They are available in several forms, each intended for a particular purpose. Nanospheres and nanocapsules are the two most prevalent

structural kinds [45] Drugs or other compounds are uniformly distributed across solid nanospheres, which have a consistent polymer framework.

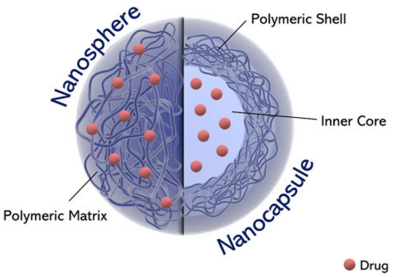

FIGURE 2.8: Biodegradable Polymeric Nanoparticles for Drug Delivery to Solid Tumors [45]

The active substance is contained in a polymer shell that encloses a liquid or solid core in nanocapsules, which have a core-shell configuration. Another distinct type of polymeric nanoparticle is dendrimers. Numerous functional groups on the surface of these extremely branched, tree-like structures enable the attachment of different medicinal substances [46]. They are frequently made for drug delivery systems which reduce the adverse effects of the drug and boost drug effectiveness. For gene therapy, polymeric nanoparticles can carry genetic material, such as DNA or RNA, into cells, presenting a viable technique for treating genetic illnesses [47].

2.6.6 Lipid-Based Nanoparticles

Lipid-based nanoparticles mainly composed of lipids, are tiny carriers for use not only in drug delivery but also in other applications because they have unique properties. They are able to penetrate into the cells efficiently and easily by encapsulating the wide range of therapeutic agents like small molecules, proteins, and nucleic acids, which increase the solubility, stability and bioavailability of molecules [48]. Moreover, the possibility of the surface modification of these nanoparticles is an efficient way to boost their surface characteristics that can be used in the treatment against different diseases and disorders that caused by the abnormality of specific cell and tissues. Hence, they can be functional. The versatility and safety profile of lipid-based nanoparticles keep them at the forefront of drug delivery and related research [49].

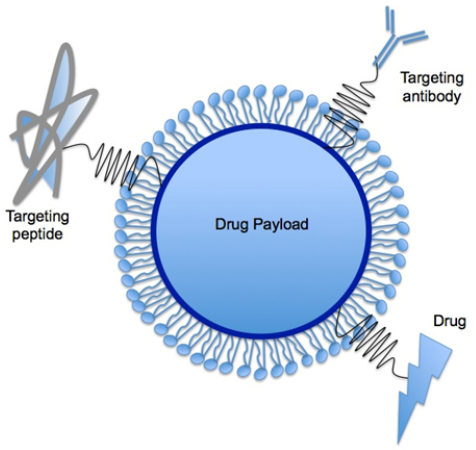

FIGURE 2.9: Lipid-based nanoparticle [48, 49]

2.7 Zinc Sulfide Nanoparticles (ZnS NPs)

Zinc sulfide nanoparticles (ZnS NPs) can be classified as the semiconductor nanomaterials which are distinguished for their exceptional optical, electrical and chemical properties, which primarily have been possible because of their small size and structure. ZnS NPs are semiconductor materials that are unique in many ways due to their brilliance (unmatched), stability, toxicity, and other factors, which make them an ideal choice for different industrial, as well as biological applications [50]. The surface of ZnS NPs can be simply modified by introducing the different functional groups, or monomers, or polymers into it, thus, functionalization that assists in drug delivery, targets specific biological markers, or improves solubility and dispersion in biological environments.

In the green synthesis of ZnS NPs, the plant extracts are utilized due to their content of bioactive compounds such as proteins, phenols, alkaloids, and flavonoids, which serve as the stabilizing and reducing agents for the synthesis of the nanoparticles [50–55]. These bioactive compounds play a role in the synthesis of zinc salts and a sulfur source as well as the stabilization of particles and maintaining their size which helps in the formation of ZnS nanoparticles. ZnS nanoparticles synthesis is done by modifying the reaction conditions such as pH, temperature, and the amount of precursor to the desired size and shape of the nanoparticles [56].

2.8 Biomedical Application of ZNS NPs

ZnS nanoparticles (NPs) have shown some antibacterial properties, making them useful in coatings and wound dressings—situations where resistance to bacteria or fungi is beneficial. Additionally, ZnS NPs exhibit notable photoluminescence; when stimulated by a light source, they emit light. Their luminescence can be tailored by doping with various metal ions resulting in different emission colors and enhanced brightness, which is crucial for tracking and imaging applications in biological systems [57]. ZnS nanoparticles (NPs) are being investigated for their role in photodynamic therapy (PDT). When exposed to light, they generate reactive oxygen species (ROS) that can effectively destroy cancer cells.

Besides, these nanoparticles may act as the carriers of chemotherapy agents to specific tumors, simultaneously saving the surrounding non-cancerous cells from damage. Because of their low toxicity, ZnS NPs can safely be applied in in vivo experiments, which could be the groundwork for potential usage in drug delivery [58]. ZnS nanoparticles can be designed to carry genetic material, e.g., DNA or siRNA, into the cells. Thus, they are of small size which allows them to penetrate the cell and be engineered to release the genetic agent responding to cellular conditions, and this is of great importance for gene therapy applications.

2.9 Green Synthesis of ZnS NPs with *Justicia adhatoda* Plant Extract

The plant's natural reducing and stabilizing potential is utilized in the green synthesis of ZnS NPs using *Justicia adhatoda* plant's extract. This process is environmentally friendly and sustainable. The plant is abundant in various phytochemicals such as flavonoids, alkaloids, and tannins, which are crucial for the production of nanoparticles [59].

FIGURE 2.10: *Justicia adhatoda* [60]

FIGURE 2.11: *Justicia adhatoda* *L* species [61]

2.9.1 Introduction and Distribution of *Justicia adhatoda*

The perennial shrub *Justicia adhatoda*, commonly referred as Malabar nut, is a member of the Acanthaceae family. This plant has been used for ages in traditional medical systems. *Justicia adhatoda*'s leaves, flowers, and roots have long been used to cure a variety of illnesses, including as bronchitis, coughs, respiratory disorders, and other inflammatory problems [60].

Native to the Indian subcontinent, *Justicia adhatoda* thrives in tropical and subtropical climates. It is commonly found in nations including Pakistan, Bangladesh, Nepal, Myanmar, India, and Sri Lanka. It prefers moist, well-drained soil. The plant usually grows in gardens, along roadsides, and in wooded places. It prefers moist, well-drained soil. It has dark green, lanceolate leaves that are about 5 to 10 cm long and can grow to a height of 1 to 3 meters. The plant attracts a variety of pollinators with its clusters of white or pale yellow flowers [61].

2.10 Medicinal Properties of *Justicia adhatoda*

Justicia adhatoda is a well-known plant that has many uses in traditional medicine systems. The leaves of *Justicia adhatoda* have anti-inflammatory and expectorant properties, so they are well known for their pharmaceutical effect that helps asthma, bronchitis and coughs.

Alkaloids, which are a kind of active constituent within the leaves of *Justicia adhatoda*, has been shown to help relax the muscles in bronchial passage and by widening the airways they facilitiate the easier breathing. This demonstrates that antibacterial and antifungal properties of *Justicia adhatoda* enable it to contribute to the essential role the plant plays in curing infections of respiratory systems [62].

In its traditional forms, the plant is used to treat various ailments because it prevents viruses and germs from growing. Such as fever, injuries and infections that affect the skin. Research shows that its potential as a natural antibacterial agent has been supported by laboratory studies of compounds in the leaves against organisms such as *Escherichia coli* and *Staphylococcus aureus*, meaning that it can be used successfully to treat pathologies caused by these pathogens.

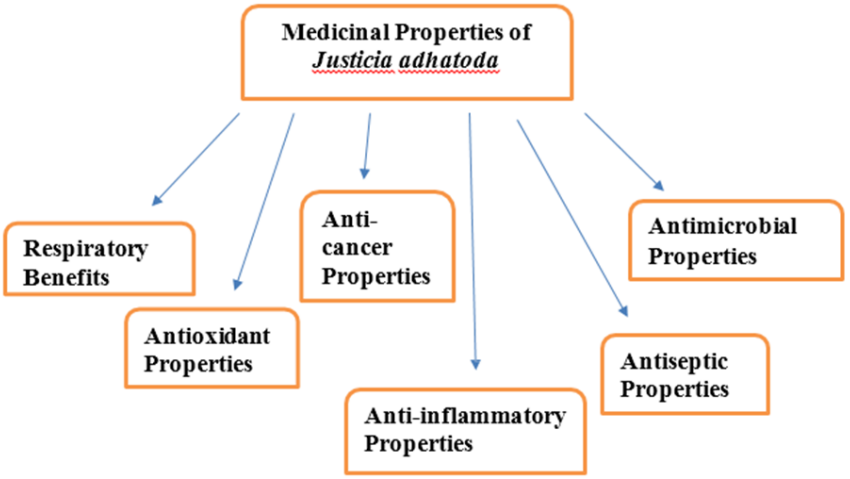

FIGURE 2.12: Flowchart representing the biomedical applications of *Justicia adhatoda* [63]

In addition, *Justicia adhatoda* is believed to possess antioxidant capabilities that can protect the body against cellular damage and counteract oxidative stress which is attributed to flavonoids and phenolics in its pigment content. It enables it

to bring even greater effectiveness to its medicinal effects. Furthermore, certain research studies suggested that *Justicia adhatoda* may help regulate blood sugar levels. It has been studied as a possible response to diabetes [63, 64].

Chapter 3

Material and Methods

3.1 Material

The materials used in this experiment were broadly comprises of different chemicals and reagents, apparatus and equipment, animal model (Sprague-Dawley rat), its blood and liver.

3.2 Chemicals

The chemicals that were used in this research are Zinc chloride ($ZnCl_2$), sodium sulfide (Na_2S), distilled water (H_2O), acetone (C_3H_6O), formalin (CH_2O), chloroform ($CHCl_3$) and magnetic stirrer.

3.3 Apparatus and Equipments

The apparatus and equipments that was used in this research are pipette Eppendorf tubes, thermometer, incubator, reaction vessels, glassware, centrifuge, beaker, magnetic stirrer, hot plate, Erlenmeyer flasks, funnels, beaker, burette, volumetric flask, graduated cylinders, calibrated digital balance, EDTA coated tubes, centrifuge machine, Falcon tubes and Culture tubes.

3.4 Ethical Considerations

The ethical review committee of Capital University of Science and Technology, Islamabad, Pakistan, approved the research titled "Safety Evaluation and in-vivo Toxicity of Green-Synthesized Zinc Sulfide Nanoparticles with *Justicia adhatoda* Extract on Rat Model". All procedures followed the committee's guidelines to ensure the ethical treatment of the animals and minimize the discomfort or stress to the rats during the study period.

3.5 Methodology

The research process outlined in the study was simply categorized into four steps. Preparation of Green –synthesized ZnS NPs using *Justicia adhatoda* plant extract, characterization of the prepared NPs, testing of prepared Green-Synthesized ZnS NPs on rat model and assessment of different biological parameters of rat.

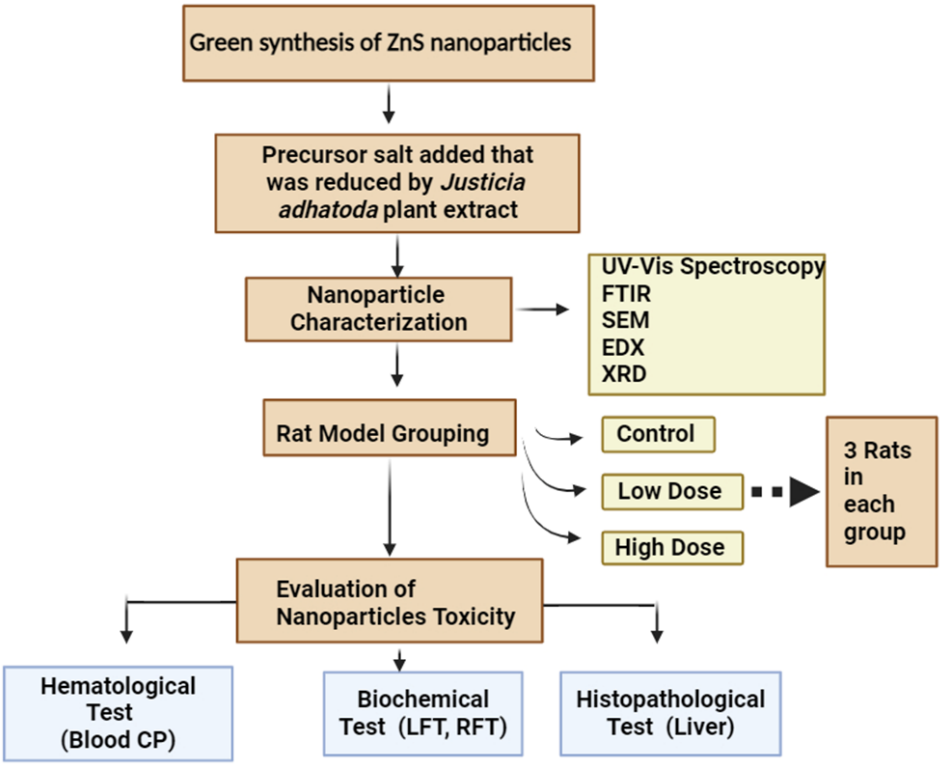

FIGURE 3.1: Methodology flow chart

3.5.1 Plant Collection and Preparation of *Justicia adhatoda* L. extract

Justicia adhatoda was sourced from the surroundings of Islamabad, the capital of Pakistan, during September 2024. The leaves and flower of plants were identified and authenticated by the Botany Department of Arid Agriculture University, Rawalpindi. Leaves of the plant were collected carefully and placed in a sterile box for storage and for transport to the laboratory. Distilled water was used to wash the fresh leaves initially and to remove any surface dust and contamination.

Justicia adhatoda leaves were dried and washed with distilled water. After drying at room temperature, the leaves were grinded into a fine powder.

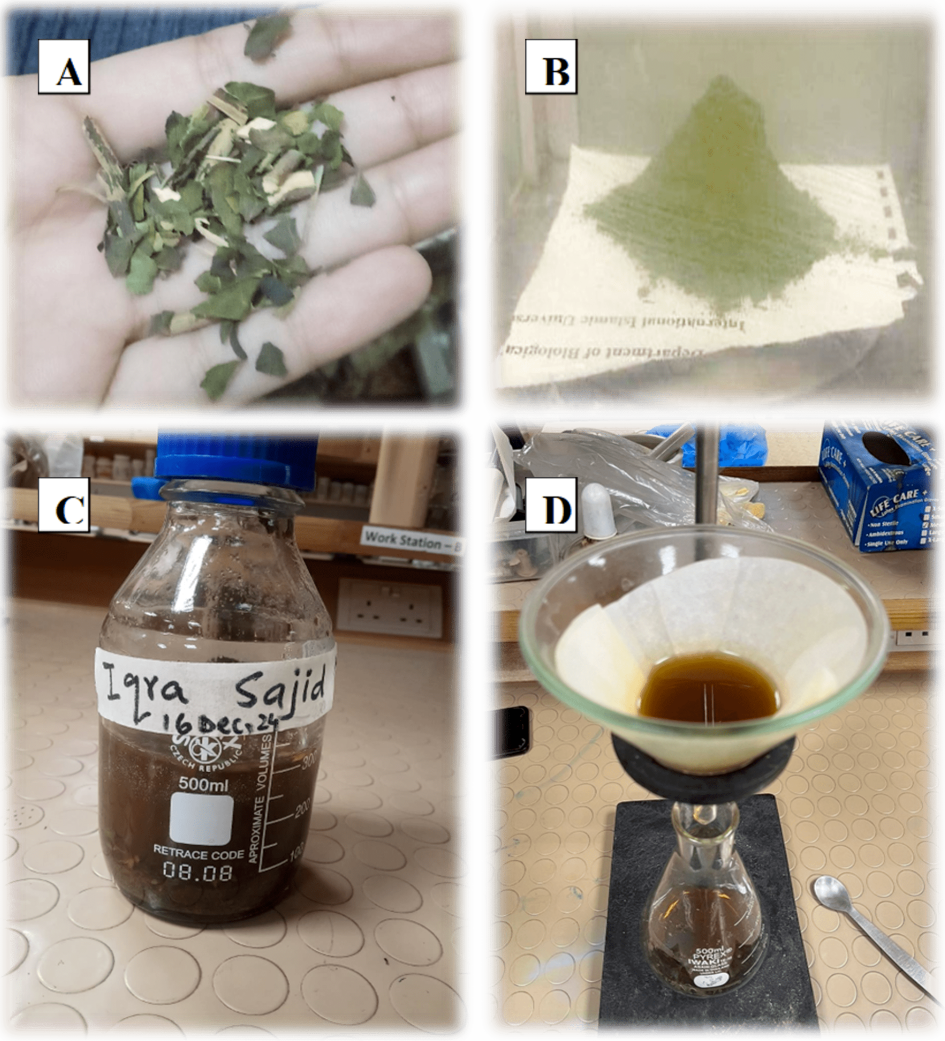

FIGURE 3.2: *Justicia adhatoda* plant extract preparation

Powdered leaves were boiled in 150 ml of distilled water for about six hours. 10g of the powder was taken and mixed in 150ml distilled water in Erlenmeyer flask. The flask was placed on magnetic stirrer at 60^{o}C for 6 hours. The extract was then cooled at room temperature. The extract was filtered by using filter paper and then stored at 4^{o}C until utilized for Zinc Chloride and Sodium sulfide reduction into ZnS NPs.

3.5.2 Synthesis of Green-synthesized ZnS NPs

3.5.2.1 Preparation of Zinc Precursor Solution

For preparing an aqueous solution of a zinc precursor, such as zinc chloride, we dissolved the compound in distilled water. This solution provided zinc ions (Zn^{2+}) needed for nanoparticle formation. We dissolved 0.1 M zinc chloride in 50 mL of distilled water.

3.5.2.2 Preparation of Sulfide Solution

On the other side we prepared the sulfide solution by dissolving 0.1 M sodium sulfide in another 50 mL of distilled water.

3.5.2.3 Mixing Plant Extract with ZnS Solution

The precursor salt of zinc chloride and sodium sulfide were mixed together followed by the addition of plant extract which reduced both salts into ZnS nanoparticles. A constant temperature (around 60-70^{o}C) for about 1-2 hours was thus maintained which allowed the complete reaction for the growth of ZnS nanoparticles.

3.5.2.4 Isolation and Purification of ZnS Nanoparticles

The solution was centrifuged at 5000 rpm for 15 minutes and we collected the precipitates of ZnS NPs. Then we gave a washing to ZnS NPs with distilled water

and ethanol several times for the removal of impurities. The ZnS NPs were dried in an oven at about 60°C. The ZnS nanoparticles were then ready for characterization and further application.

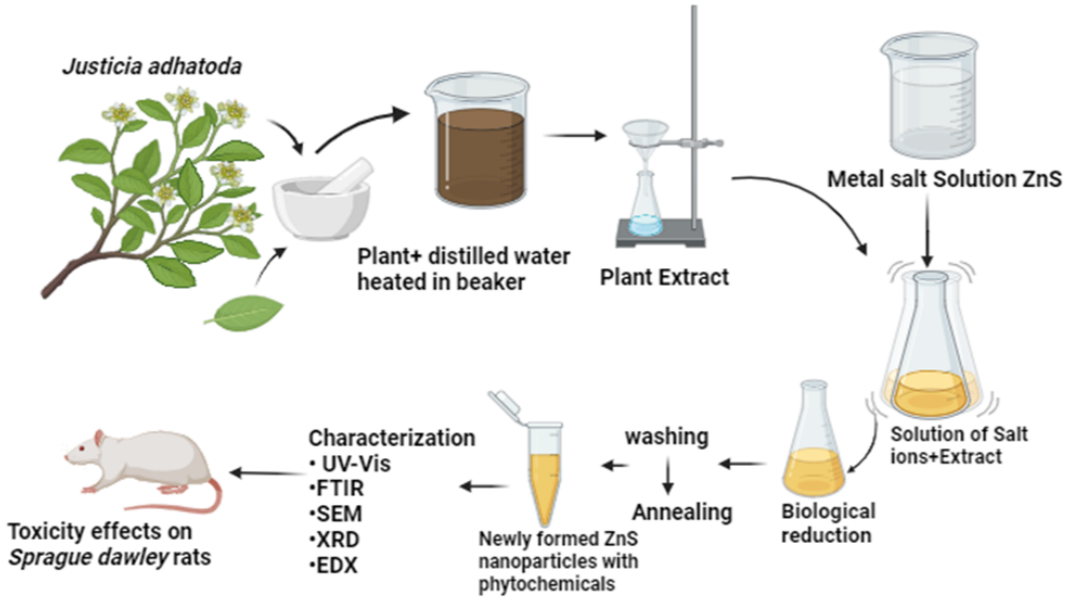

FIGURE 3.3: Schematic diagram of green synthesis of Zinc Sulfide nanoparticles with *Justicia adhatoda*

3.6 Yield of Green- Synthesized ZnS Nanoparticles

The yield of ZnS NPs was calculated as:

$$(\%)\ Nanoparticles\ Yield\ =\ \frac{W1}{W2} \times 100$$

Where,

W1 = Nanoparticles formed and

W2 = Salt used in reaction

3.7 Physicochemical Characterization of ZnS Nanoparticles

ZnS nanoparticles were systematically characterized by IST, Islamabad. Numerous physicochemical techniques like UV-Visible spectroscopy (UV Vis Shimadzu UV-1800), X-ray diffraction analysis (XRD) (RD 50, GNR Explorer), fourier-transform infrared spectroscopy (FTIR) (PerkinElmer) and scanning electron microscope (SEM) and energy dispersive X-ray analysis (EDX) (MIRA 3, TESCAN) revealed the identification, phase composition, crystallite structure, and size of ZnS nanoparticles [65].

3.7.1 Fourier Transform Infrared (FTIR) Spectroscopy

It is used for functional group analysis of nanoparticles. Nanoparticles has its own surface chemistry. It has functional groups/ chemical groups on its surface. By using this technique the functional groups present in the nanoparticles were identified [66].

3.7.2 Ultraviolet-Visible (UV-Vis) Spectroscopy

This characterization technique was used for initial screening of ZnS nanoparticles [67]. The chemical components included in the nanoparticles were analyzed both qualitatively and quantitatively using ultraviolet-visible (UV-Vis) spectroscopy.

3.7.3 X-Ray Diffraction (XRD)

The crystalline nature of the nanoparticles and the purity of nanoparticle were confirmed by X-Ray Diffraction (XRD) examination. This method worked well for understanding the structural properties of ZnS NPs [68].

3.7.4 Scanning Electron Microscopy (SEM)

The size and morphological characteristics of the individual Zn nanoparticles were seen via scanning electron microscopy (SEM) imaging. This was important information regarding the general form and dimensional properties of the produced ZnS nanoparticles [69].

3.7.5 EDX (Energy-dispersive X-ray Spectroscopy)

The elemental composition of nanoparticles and relative weights and percentages of the elements were identified by Energy- dispersive X-ray spectroscopy. EDX was used to detect any type of impurities or additional elements, such as oxygen or carbon, in the formed ZnS NPs [70].

3.8 Animal Selection and Acclimatization

Nine young adult male Sprague-Dawley rats were selected for the experiment. Their average weight was 200-250gm (six to eight weeks old). They were taken from the Department of Pharmacy, CUST, Islamabad. These rats were kept in animal house with regulated room temperature (60–70% relative humidity) [71]. Temperature was maintained at 22 ± 2 in celsius scale, with humidity of 55% ± 10%, and 12 hours of light and dark cycle [71]. During the first week, all rats were undergo acclimatization to the animal house environment to minimize stress and ensure consistent baseline measurements.

3.9 Experimental Groups

Nine rats were selected for our three experimental groups (control group, low dose group, high dose group) for a period of 28 days. The rats had an unrestricted access to water and fed a normal laboratory meal. The division of rats for each group was as:

- **Group 1**: It was a control group and were given diet and water under normal conditions for 20 days of study period [73].
- **Group 2**: It was a low dose taking group of ZnS NPs with a diet and water under normal conditions for 20 days of study period [73]
- **Group 3**: It was a high dose taking group of ZnS NPs with a diet and water normal conditions for 20 days of study period [73]

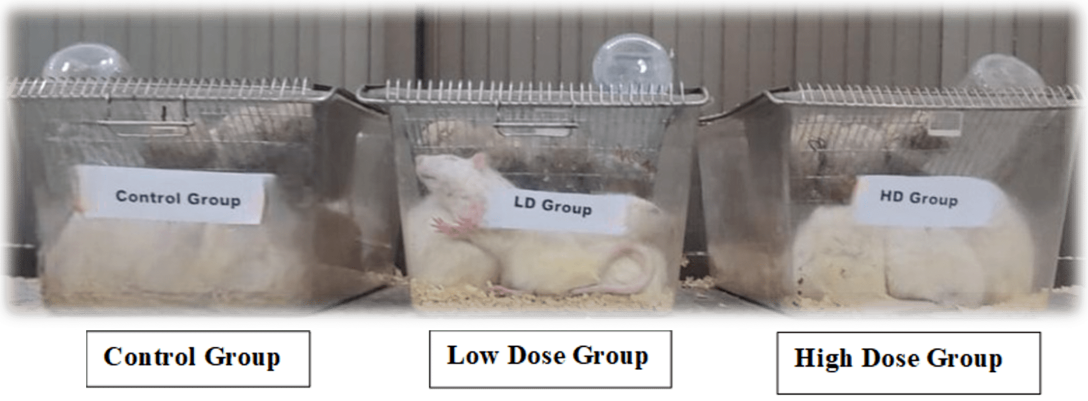

FIGURE 3.4: Sprague-Dawley rats categorized into 3 groups according to experimental design [73]

3.10 Dose Description of ZnS NPs

Table 3.1 shows dose description of ZnS NPs. The average weight of the rat was 200gm. Dose preparation of ZnS NPs was decided on the basis of tolerate dose of CuS NPs which was 8.66 mg/kg [74]. On the basis of tolerate dose the dosage were decided as 1.73 mg/200gm (low dose taking group) and 3.46mg/200gm (high dose taking group) [74].

TABLE 3.1: Dose preparation of ZnS NPs on the basis of tolerate dose of CuS NPs [74]

Average rat weight	200gm
Low dose of ZnS NPs	1.73 mg/200gm
High dose of ZnS NPs	3.46mg/200gm

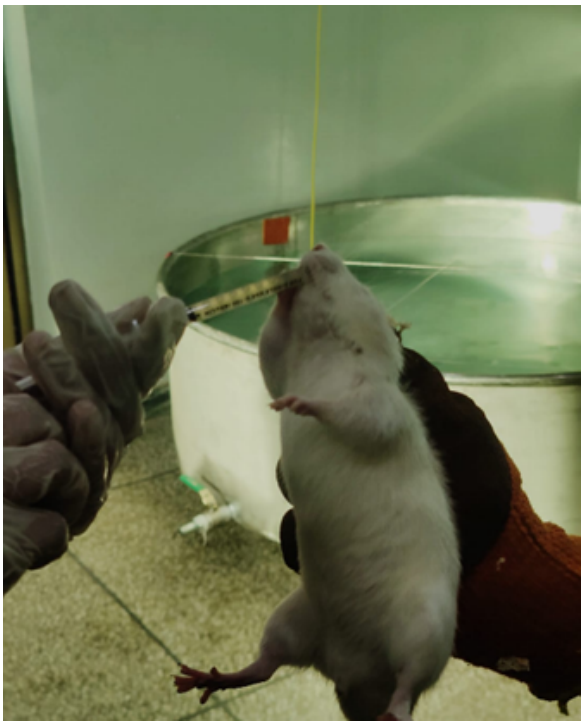

FIGURE 3.5: Rat being given Green-Synthesized ZnS NPs dose with feeding tube

3.11 Morphological Assessment (Body Weight)

The weights of all the rats included in our experimental group were measured initially and then on regular basis from the dosage day till the end of the study period of 20 days. An electronic balance was used for the weights measurement. The values were noted to make a comparison with control group [75].

3.12 Animal Dissection

All the rats were dissected on the 21^{st} day and chloroform was used for making them anaesthetized. The rats were killed by cervical dislocation. The liver was dissected out and tissues were transferred to formaldehyde solution for preservation and stored in -70^o freezer [76]

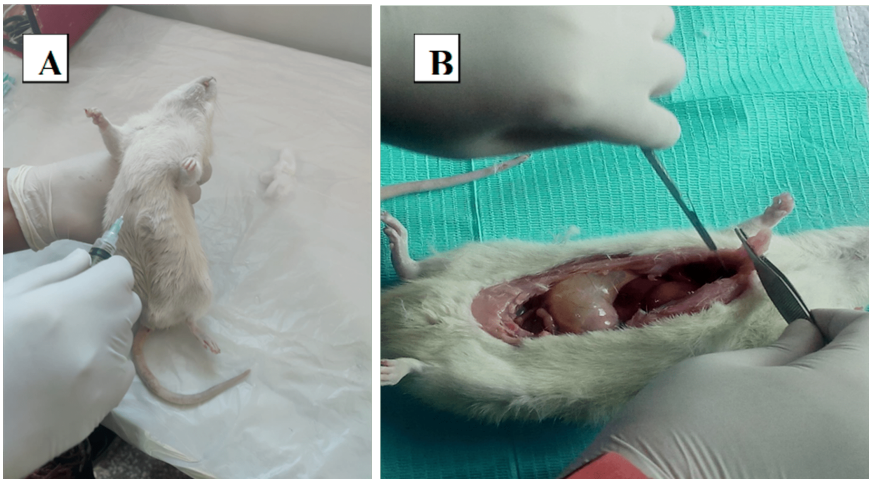

FIGURE 3.6: Dissection of Rat

3.13 Hematological Analysis

After 20 days the blood sampling of all the rats were done by cardiac puncture and blood was collected in EDTA-coated tubes for Hematological assessment.

The parameters that were checked in after hematological analysis were: red blood cells (RBC), white blood cells (WBC), platelets/thrombocytes (PLT), hemoglobin (Hb), Hematocrit (HCT), mean corpuscular volume (MCV), mean corpuscular hemoglobin concentration (MCHC), lymphocytes (LYMPHO), monocytes (MONO), eosinophils (EOS), and neutrophils (NEU), mean corpuscular hemoglobin (MCH) [77–80].

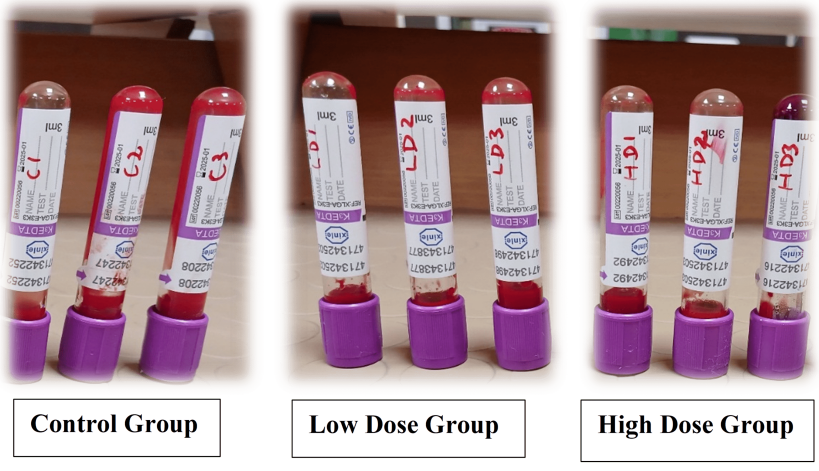

FIGURE 3.7: Blood sample collection for hematological analysis

3.14 Biochemical Analysis

For serum biochemical examination Blood sampling was done after giving anesthesia. The serum was used to measure the biochemical parameters i.e, liver function test (LFT) and renal functioning test (RFT) [81].

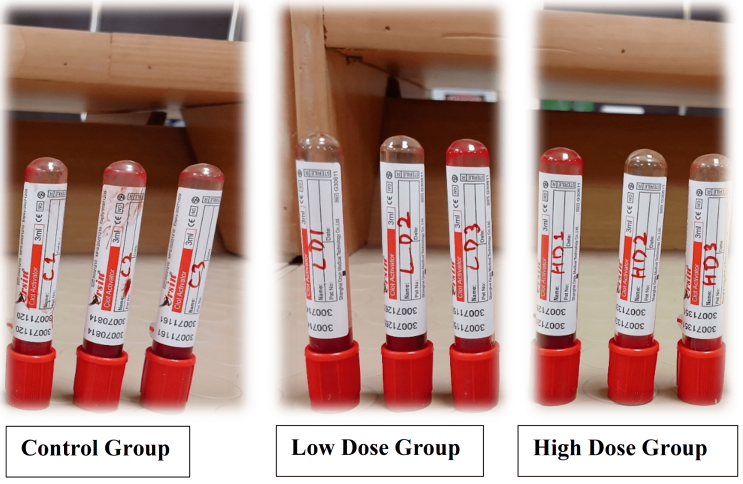

FIGURE 3.8: Blood sample collection for biochemical analysis

3.15 Histopathology Study

The animals were sacrificed for histopathological examinations. Rat liver was preserved in 10% formalin for histopathological analysis [82].

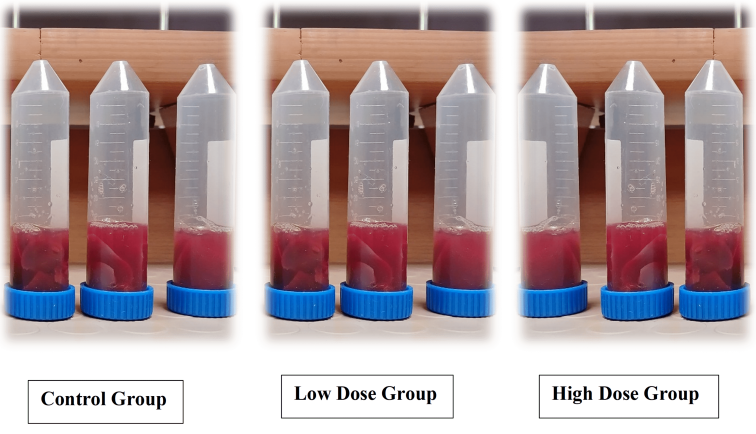

FIGURE 3.9: Liver sample collection for Histopathological analysis

3.16 Statistical Analysis

Statistical analysis employed a one-way analysis of variance (ANOVA) to assess differences between groups [83]

Chapter 4

Results and Discussion

4.1 Plant Extract & Green-Synthesized ZnS Nanoparticles Synthesis

In this study, extract of *Justicia adhatoda* plant was used to initiate the synthesis of green-synthesized zinc sulfide (ZnS) nanoparticles. The extract was prepared from the aerial parts of the *Justicia adhatoda* plant in 150 ml of distilled water, followed by filtration that resulted in light brown to brown colours shown in (Fig 4.1A).

A 0.1 M zinc chloride ($ZnCl_2$) and sodium sulfide (Na_2S) solution was prepared in 50 ml of distilled water, mixed together and added drop wise to the plant extract. A constant temperature (around 60-70^{o}C) for about 1-2 hours was thus maintained which allowed the complete reaction for the growth of ZnS nanoparticles.

Bioactive compounds such as polyphenols and flavonoids in the extract acted as reducing agents, reducing the precursor salts to form ZnS nanoparticles. The color changed from dark brown to pale yellow indicated the synthesis of Green –synthesized ZnS nanoparticles (Fig 4.1B) [84]. Functional groups in the plant extract acted as stabilizers, preventing aggregation and maintaining the colloidal properties of the green synthesized ZnS nanoparticles.

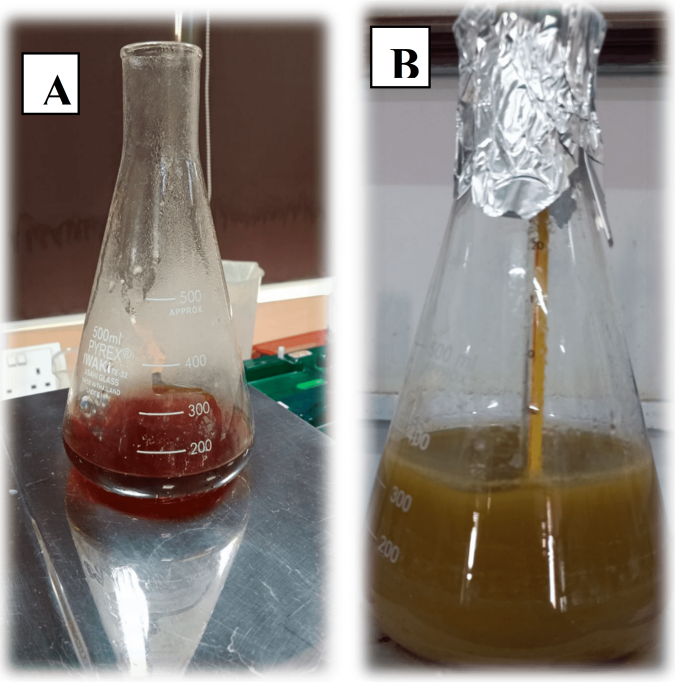

FIGURE 4.1: A. Synthesized extract of the *Justicia adhatoda* plant, B. Color change indicated of plant extract when mixed with Zinc Sulfide Solution

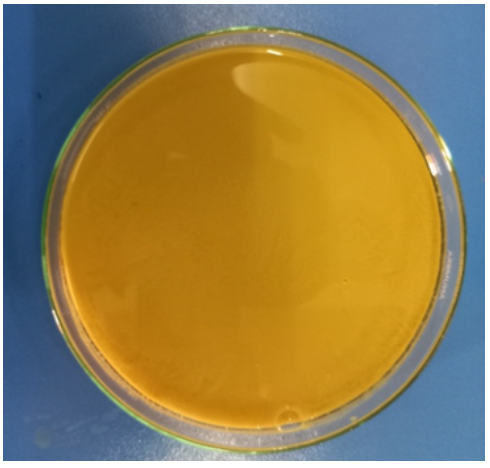

FIGURE 4.2: Color change to pale yellow indicating the synthesis of Green – synthesized ZnS NPs

4.1.1 Green-Synthesized ZnS Nanoparticles after Washing and Drying

The dried Green- Synthesized ZnS nanoparticles washed with distilled water and ethanol several times for the removal of impurities. The NPs were dried in an

oven at about 60^{o}C. The ZnS nanoparticles are now ready for characterization and further application.

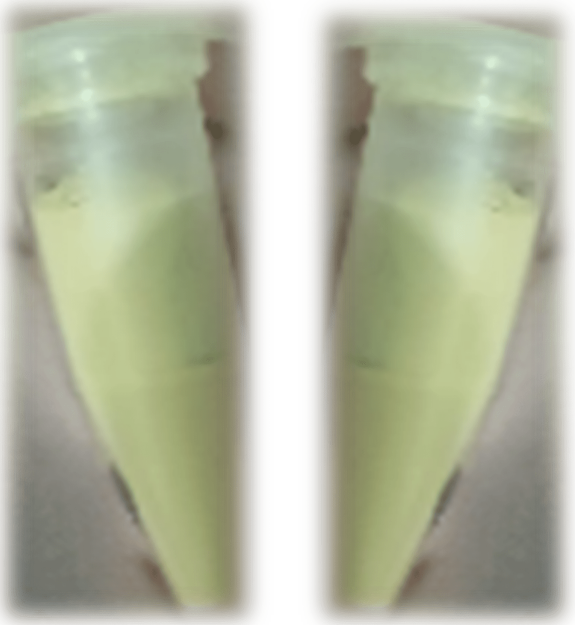

FIGURE 4.3: Green- synthesized Zinc sulfide (ZnS NPs) after washing and drying

4.1.2 Yield

Table 4.1 shows that the temperature, pH and reaction time affect the yield of Green- Synthesized ZnS-NPs. The optimum pH required for the synthesis of ZnS was 8 with 65 ^{o}C optimum temperature and 4h of reaction time.

TABLE 4.1: Yield of green synthesized ZnS NPs

NPs	**Precursor salts ,W2 (g)**	**Optimum PH**	**Temperature (^{o}C)**	**Reaction Time (hours)**	**NPs attained, W1 (g)**	**Average Yeild (%)**
Green Synthesized ZnS NPs	$ZnCl_2$, N_2S(1.7g)	8	65^{o}C	4h	0.39g	22.94%

4.2 Physicochemical Characterization of Green-synthesized ZnS Nanoparticles

4.2.1 SEM

The size and morphological characteristics of the individual Zn nanoparticles was seen through scanning electron microscopy (SEM) imaging as shown in figure. This provide important information about the general form and dimensional properties of the synthesized ZnS nanoparticle [85]. The SEM micrograph of Green- synthesized ZnS NPs show spherical shaped morphologies of nanoparticles and showed that they have good homogeneity and separation. Precipitation may also be observed in the SEM images of ZnS NPs which shows the successful synthesis of Green synthesized ZnS. The results also show that the average size range of green synthesized zinc sulfide Nanoparticles is between 73nm [85].

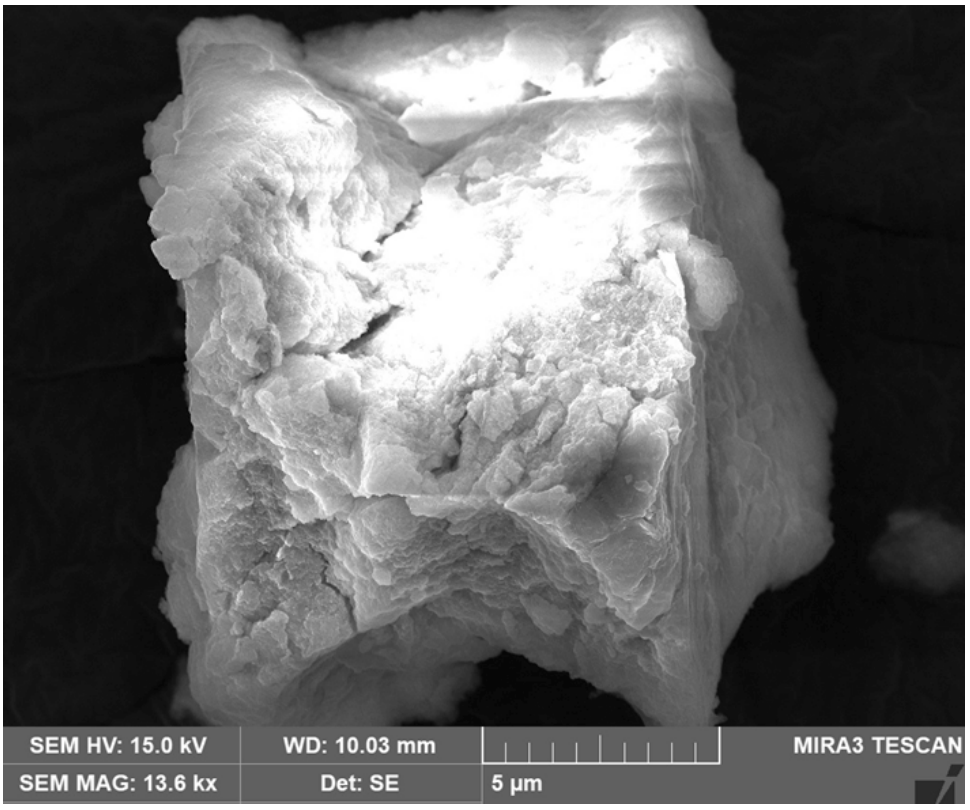

FIGURE 4.4: SEM images of Green synthesized Zinc sulfide nanoparticles at 5μm

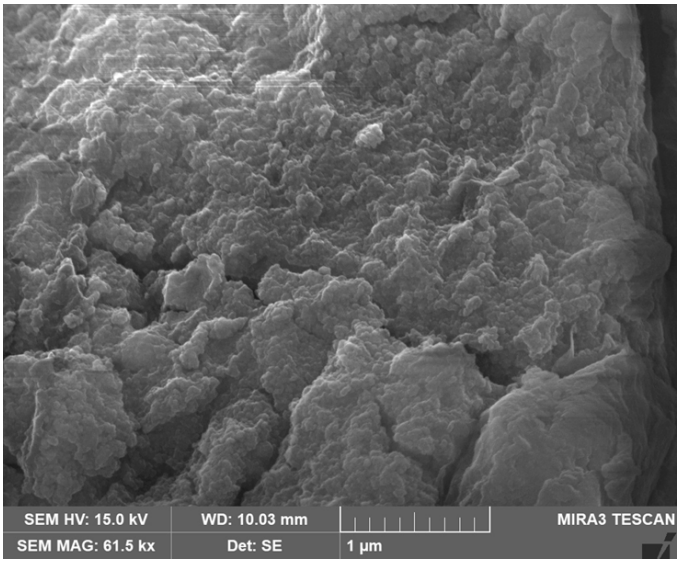

FIGURE 4.5: SEM images of Green synthesized Zinc sulfide nanoparticles at 1μm

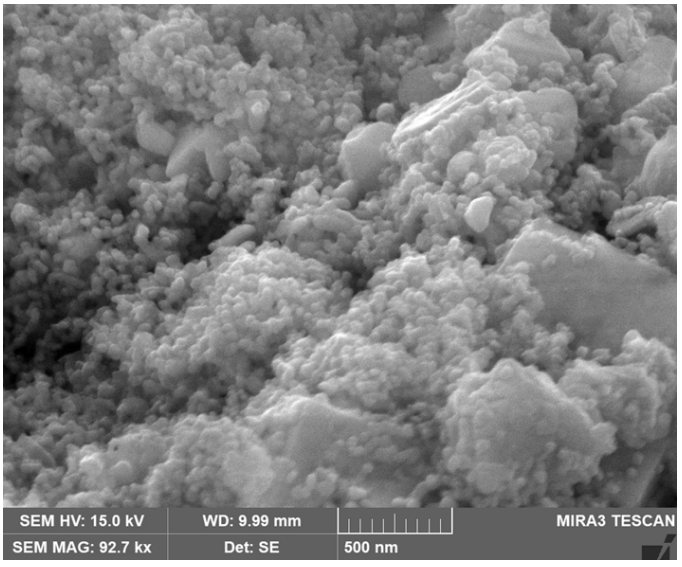

FIGURE 4.6: SEM images of Green synthesized Zinc sulfide nanoparticles at 500nm

4.2.2 EDX

It tells us the elemental composition of nanoparticles and relative weights and percentages of the elements. EDX is used to detect the presence of any impurities or additional elements, such as oxygen or carbon, in the formed ZnS NPs [86]. The elemental analysis indicated the atomic and mass percentage of Zn, Cl, S and Na (fig 4.2). It represents the atomic proportion of Zn, Cl, Na, S, O, Si, P and C with

45.73%, 0.24%, 4.82%, 17.62%, 21.04%, 0.22%, 0.49% and 11.85% respectively. The mass proportion of Zn, Cl, Na, S, O, Si, P and C were shown as 39.12%, 0.15%, 1.64%, 17.88%, 22.95%, 0.175%, 0.35% and 15.74% respectively (Table 4.2). It shows the high presence of Zn. No major peak in the spectra indicates the purity of sample [87].

TABLE 4.2: Elemental Analysis of Green-Synthesized ZnS NPs

Element	**Line Type**	**Atomic %**	**Weight %**
Carbon	K series	11.85%	15.74%
Oxygen	K series	21.04%	22.95%
Sodium	K series	4.82%	1.64%
Silicon	K series	0.22%	0.175
Phosphorus	K series	0.49%	0.35%
Sulfur	K series	17.62%	17.88%
Chlorine	K series	0.24%	0.15%
Zinc	L series	45.73%	39.12%
Total:		100.00	100.00

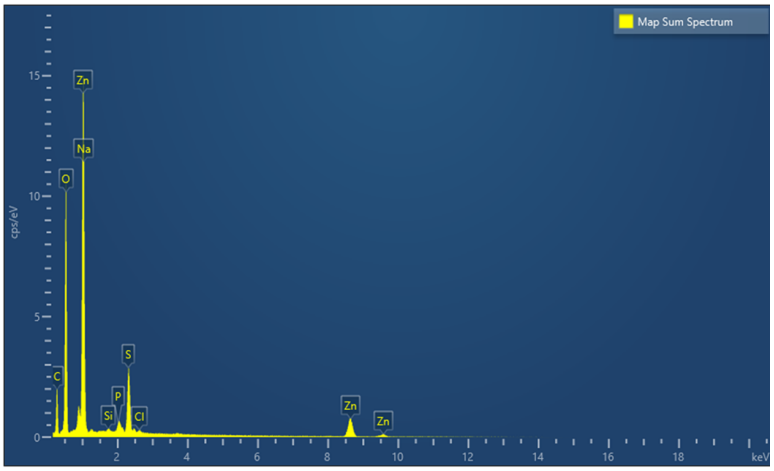

FIGURE 4.7: EDX spectra of ZnS NPs

4.2.3 FTIR

FTIR was used to identify the composition of functional groups of *Justicia adhatoda* plant extract and ZnS nanoparticles. The IR bands of plant extract were measured in the range of 500–4000 cm^{-1} and IR bands of ZnS NPs were measured in the range of 400–5000 cm^{-1} [88]. The spectra of ZnS NPs showed eminent

peaks at 3386.77, 2895.69, 1597.85, 1597.85, 1045.38 and 492.92 cm^{-1} respectively shown in the fig 4.8. While the spectra of *Justicia adhatoda* plant extract showed eminent peaks at 3271.5, 2896.5, 1695.5, 1421.2, 1064.5 and 854.2 cm^{-1} as shown in figure 4.9.

Table 4.3 shows the interpretation of FTIR data that distinct bands were observed in NPs and plants which represent O-H stretching (Alcohol), C-H stretching (Alkanes), C-H stretching, C=C stretching, O-H stretching, C-O stretching, O-H bonding, C-O stretching, ZnS stretching Vibrations and C-H bending respectively. The FTIR spectra shows peaks that correlate to ZnS [88]

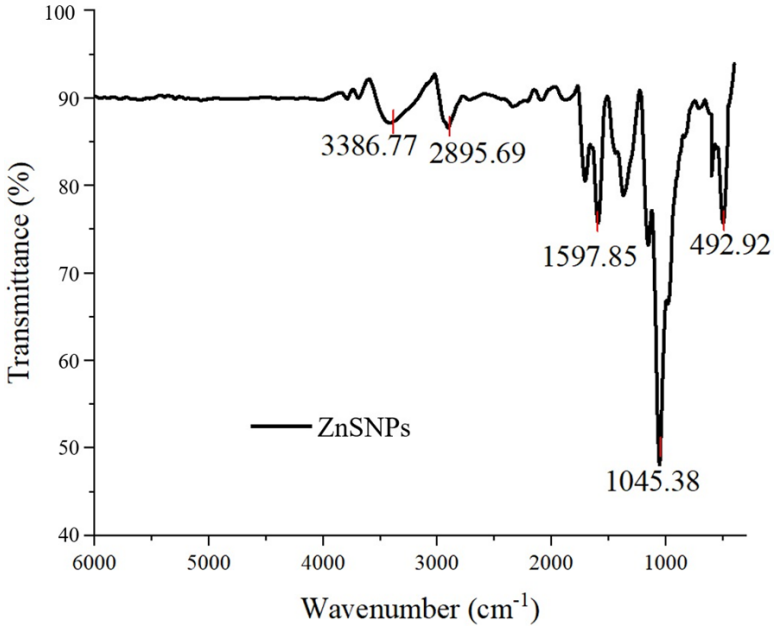

FIGURE 4.8: FTIR Spectra of Zinc sulfide nanoparticles

The peak values 436-631 cm^{-1} confirms the ZnS Vibrations. The range 3550-3200 cm^{-1} correlate to O-H stretching from alcohols or phenols. The band at 3386.77 cm^{-1} represents the hydroxyl groups on the nanoparticle surface may be due to adsorbed water or surface functionalization. The peak at 2895.69 cm^{-1} also corresponds to O-H stretching, representing the hydroxyl groups in plant-derived compounds. The peaks range 2000-1650 cm^{-1} correlate to C-H bending vibrations in aromatic compounds. The band at 1597.85 cm^{-1} represents that aromatic structures from plant extract are adsorbed on the nanoparticle surface [89]. The band at 3386.77 cm^{-1} as ZnS more effectice in adsorption-based applications.

sociated to OH Stretching indicating the presence of hydroxyl groups on ZnS surface making The presence of ZnS stretching vibrations at around range 459 cm^{-} , C=C stretching at band 1597.85 showing the synthesis of ZnS NPs. The results shows the synthesis of ZnS NPs.

The functional groups present in the plant extract were strong interacted on with ZnS NPs surface, and leading towards the reducing size of spherical NPs [90]. These molecules were involved in the capping of ZnS NPs and thus prevent aggregation. The band positioned at 3271.5 are due to C-H Stretching vibrations (Alkanes). C-O stretching at peak range 1085-1050 cm^{-1} near band 1054.38 in ZnS is associated with the surface carboxyl groups that can interact with plant biomolecules through Hydrogen bonding.

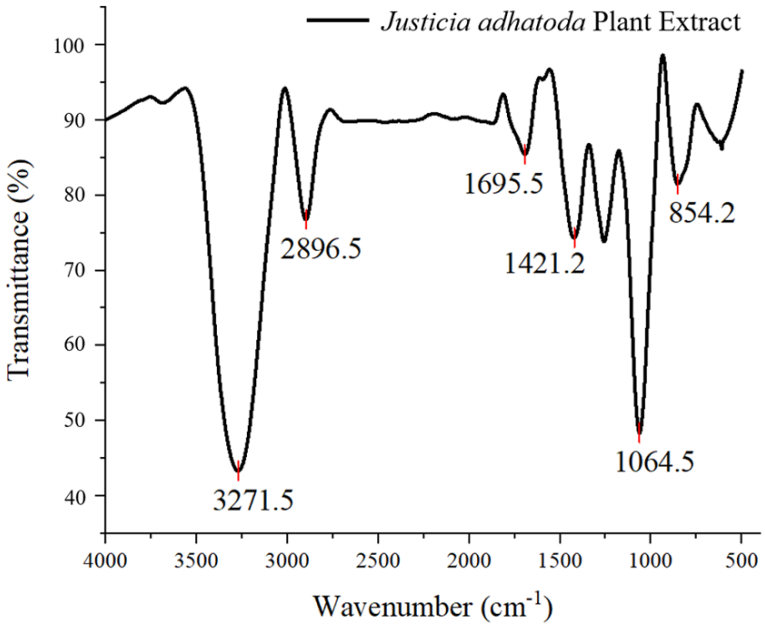

FIGURE 4.9: FTIR of the *Justicia adhatoda* plant extract

TABLE 4.3: Interpretation of the peaks obtained via FTIR spectra of Plant and Zinc sulfide nanoparticles

S.No	**Wave numbers Range (cm^{-1})**	**Frequency (cm^{-1})**	**Functional group interpretation**
1	3550-3200	3386.77 (NP)	O-H Stretching [88] Hydoxyl group (Alcohol)
2	3550-3200	3271.5 (Plant)	C-H Stretching [89] (Alkanes)

Continued on next page

Table 4.3 (continued from previous page)

S.No	Wave numbers Range (cm^{-1})	Frequency (cm^{-1})	Functional group interpretation
3	3000-2840	2896.5 (Plant)	O-H Stretching [90] Hydoxyl group (Alcohol)
4	3000-2840	2895.69 (NP)	C-H Stretching (Alkanes) [90]
5	2000-1650	1597.85 (NP)	C-H Bending [91] (Aromatic Compound)
6	2000-1650	1695.5 (Plant)	C-H Bending [88] (Aromatic Compound)
7	1650-1566	1597.85 (NP)	C=C Stretching [91] Cyclic Alkene
8	1500-1400	1421.2 (Plant)	C–C Stretching (in–ring) [89] Aromatics
9	1085-1050	1054.38 (NP)	C-O Stretching [92] (Primary Alcohol)
10	1085-1050	1064.5 (Plant)	C-O Stretching [93] (Primary Alcohol)
11	900-675	854.2 (Plant)	C-H 'Oop''Aromatics [89]
12	600-420	∼492.92 (NP)	ZnS Stretching vibrations [89]

4.2.4 XRD

The crystalline nature of the nanoparticles and the purity of nanoparticle was confirmed by X-Ray Diffraction (XRD) examination. This method works well for understanding the structural properties of ZnS NPs. The crystalline nature and purity of ZnS NPs were identified by X-ray diffraction patterns [94]. The spectrum represents the crystalline structure of ZnS nanoparticles. The graph below represents the XRD pattern of ZnS NPs for 2^o values in range of 20^o to 60^o. The largest peak of ZnS NPs was observed at the 2^o values of $\sim 30^o$ corresponding to (200) plane and at 2^o values of 27^o corresponding to (101) plane the smallest peak was observed. The longest and sharpest peak at 200 depicts the crystalline orientation of ZnS. Other peaks are at (100), (101), (102) and (103) indicating multiple crystallographic planes. At the reaction, no impurities were detected which indicates the high purity of synthesized ZnS nanoparticles. The (103) plane at 60^o confirms the structural stability of ZnS at nano scale [87].

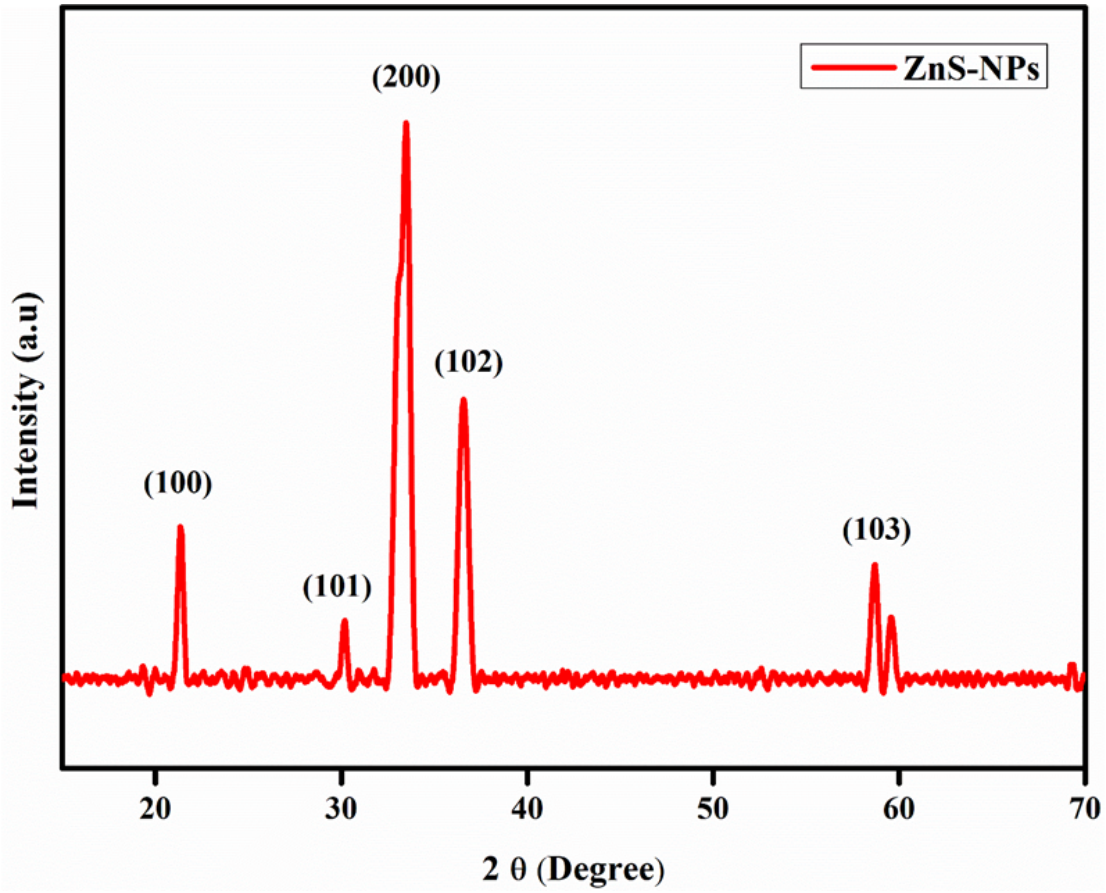

FIGURE 4.10: XRD spectra of ZnS NPs

4.2.5 UV-Visible Spectroscopy

Ultra violet- Visible spectroscopy was used for initial screening of ZnS nanoparticles [95]. The chemical components in the nanoparticles were analyzed both qualitatively and quantitatively using ultraviolet-visible (UV-Vis) spectroscopy. The green synthesized ZnS NPs was characterized by UV-Visible spectro photometer. UV-visible spectroscopy shows the absorbance spectra that is at visible range. It is represented in form of a plot of optical absorbance of wavelength [96]. The green synthesized ZnS nanoparticle was further characterized by UV-visible spectro photometer. The absorbance range was set from 200 to 800 nm. The absorption peak was observed at 291nm. (Fig 4.11), According to the research study the absorbance range of ZnS NPs was observed around 290-330nm. Therefore the maximum peak at 291nm confirms the existence of ZnS nanoparticles [96, 115].

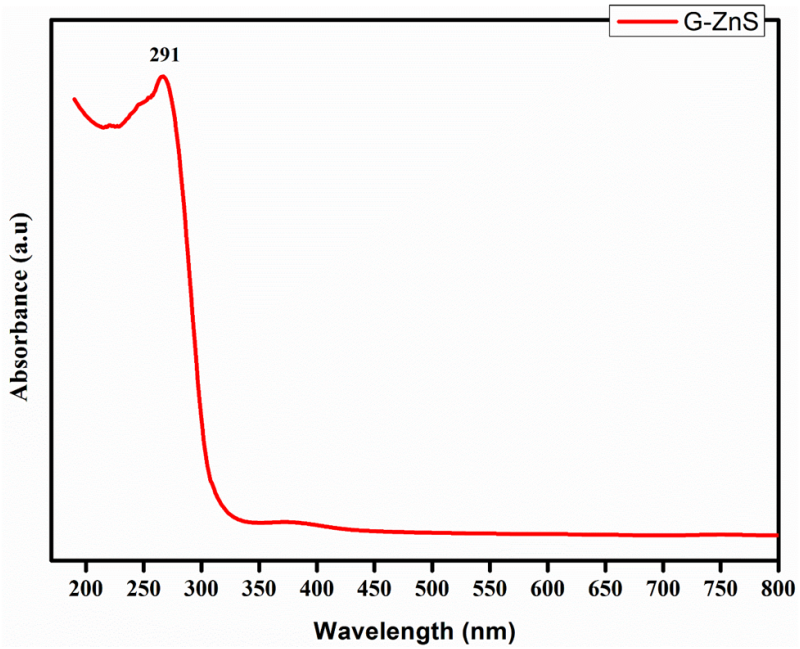

FIGURE 4.11: UV-vis spectrophotometer of green synthesized Zinc Sulfide nanoparticle

4.3 Body Weight

Body weight is an important analysis during 20 days of experiment. The weight of the control group rats were increased gradually till the end of the study but a sudden increase in weight of the low dose group and high dose group from second week onwards were observed clearly during the study period of 20 days [97].

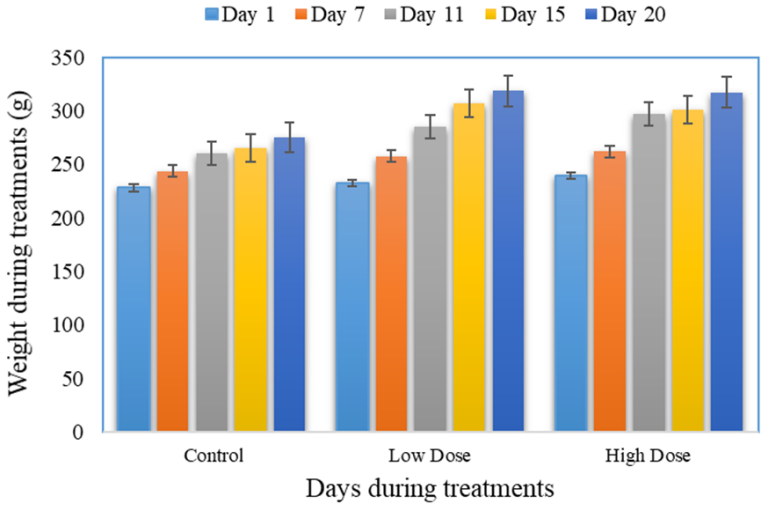

FIGURE 4.12: Weight of all groups during 20 days of experiment

The weight of the control group gradually increased during 20 days of experimental study from 228±16 to 275.33±14.97. In comparison, the weight of the low dosage group rats were increased gradually during first 7 days of experiment from 232.33±14.29 to 257.66±22 and at 14 and 20 day of experiment it was increased from 306.66±24.19 to 318.66±25 respectively. Similarly in high dose group the weight is significantly increased during 14 days from 239.33±16.77 to 300.66±59.13 and at 20 day it was increased from 300.66±59.13 to 317.33±48.34. That mean low and high dosage rats were affected more as compared to the control group and their body weight rapidly increased during the study period as compared to control group rats.

TABLE 4.4: Low dose and high dose group weight measurements in comparison with control group in one way ANOVA along Mean±SD when p-value was <0.05

Groups (n=3)	**Day 1**	**Day 7**	**Day 11**	**Day 15**	**Day 20**
Control	228±16	243.66±14.57‘	260±19.07	265.33±16.16	275.33±14.97
Low Dose	232.33±14.29	257.66±22	285.33±33.72	306.66±24.19	318.66±25
High Dose	239.33±16.77	262±23.30	297.33±43.18	300.66±59.13	317.33±48.34

4.4 Hematological Analysis

4.4.1 WBC Count

Leukocytes, also known as white blood cells or WBCs, are part of the immune system that protect the body against pathogens attack and harmful foreign substances [98]. When there is any inflammation or infection in the body, the number of white blood cells increases. When the results are compared with control group there was gradually increase of WBC count in low dose and high dose group respectively. The p value 0.004<0.01, which shows the results are very significant.

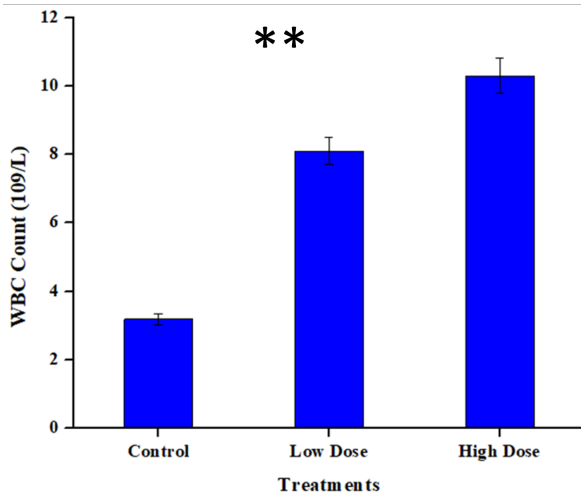

FIGURE 4.13: WBC count (1000/mm^3) of all groups, when p value was <0.05

4.4.2 RBC

Red blood cells (RBCs), erythrocytes are significant components of the circulatory system having a role of transporting oxygen from the lungs to various tissues and organs in the body [99].

RBC count in high dose group was reduced which increases the risk of inadequate oxygen supply to body results in anemia, fatigue and shortness of breath and it is the sign of certain health disorder but the RBC count in low dosage group rat is low as compared to control group, an unnoticeable change occurred. The p value 0.373>0.05, which shows the results are non-significant.

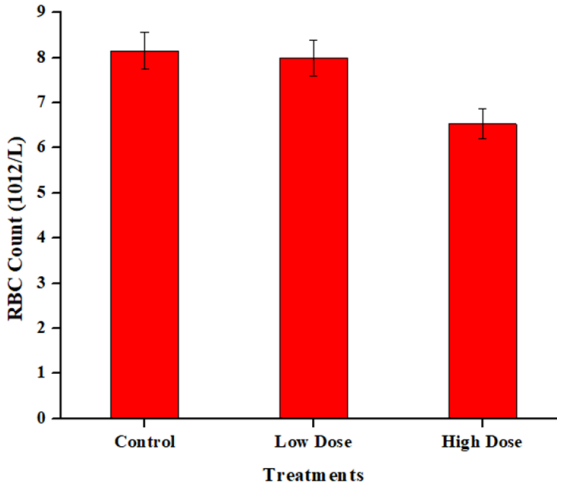

FIGURE 4.14: RBC count (mil/mm^3) of all groups, when p value was <0.05

4.4.3 Haemoglobin

Red blood cells (RBCs) contain an important essential protein hemoglobin, who function as carrying oxygen from lungs to all of the body's tissues, organs and helping to expel carbon dioxide [100]. The Hb value was higher in the low dosage group and slightly lower in the high dose group when compared to the control group. The p value 0.238>0.05, which shows the results are non-significant.

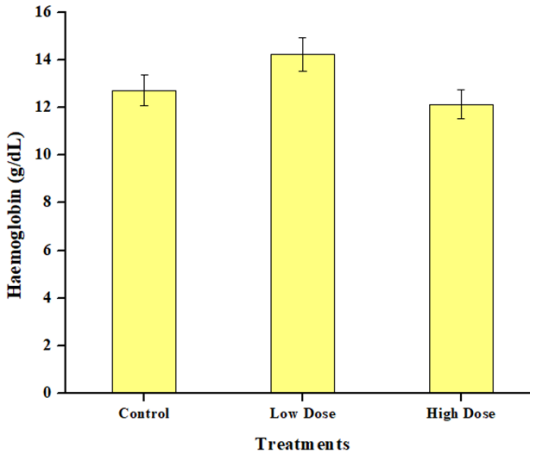

FIGURE 4.15: Haemoglobin level (g/dl) of all groups, when p value was <0.05

4.4.4 Hematocrit

It shows the percentage of red blood cells in total blood volume. It provides important details about the blood's general health and ability to deliver oxygen [101].

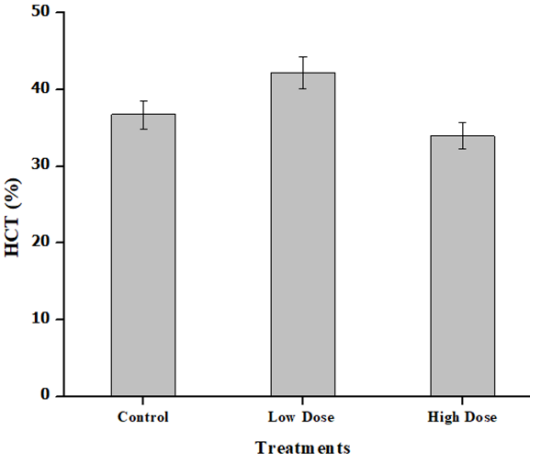

FIGURE 4.16: Hematocrit level (%) of all groups, when p value was <0.05

Hematocrit progressively increased in the low dosage group and slightly decreased in the high dose group when compared to the control group. The p value 0.346>0.05, which shows the results are non-significant.

Hematology of low and high dose group were compared with control group, in which WBC count of control group is 3.18±0.24 as comparison to WBC count of ZnS NPs dosage groups were 8.11±2.01 and 10.31±1.75 respectively which means WBC count is high in high dose and low dose groups as compared to control.

The RBC count of control group was 8.15±0.50 as compared to the low and high dose show RBC count 7.99±0.89 and 6.53±2.24 respectively which means the RBC count is slightly lower in low dose but vigorously Low in high dose group.

The Hb value in rats of control group was 12.73±0.35 but in low and high dosage groups it is slightly higher 14.23±0.97 and 13.26±1.10 respectively. The hematocrit value of control group was 36.73±2.28 but in ZnS NPs taking dosage groups (low and high) it was 42.20±2.58 and 33.96±10.59 respectively which means this hematology parameters show thickening of blood called polycythemia and reduced circulation efficiency in low dose group while anemia conditions in high dose group due to low RBC Count and decrease hematocrit as compared to control.

TABLE 4.5: WBC, RBC, Haemoglobin and hematocrit in three experimental groups in one way ANOVA with Mean±SD when p<0.05

Group Treatment (n=3)	**WBC Count**	**RBC Count**	**Haemoglobin**	**Hematocrit**
Control	3.18 ± 0.24	8.15 ± 0.50	12.73 ± 0.35	36.73 ± 2.28
Low Dose	8.11 ± 2.01	7.99 ± 0.89	14.23 ± 0.97	42.20 ± 2.58
High Dose	10.31 ± 1.75	6.53 ± 2.24	13.26 ± 1.10	33.96 ± 10.59

4.4.5 MCV

The Mean Corpuscular Volume (MCV) measures the average volume of a single red blood cell. It is an important part of a complete blood count (CBC) and gives

significant details about red blood cell dimensions [102]. The p value 0.456>0.05, which is non-significant.

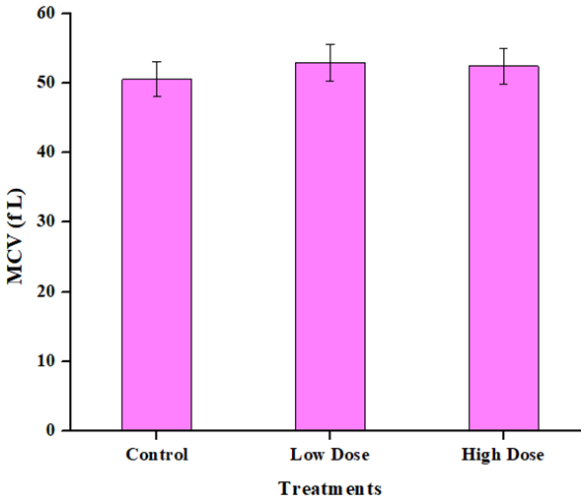

FIGURE 4.17: MCV (fl) level of all groups, when p value was <0.05

4.4.6 MCH

The Mean Corpuscular Hemoglobin (MCH) is a significant component of a complete blood count, offers information regarding the average amount of hemoglobin present in each red blood cell. MCH plays a key role in assessing the hemoglobin content within individual erythrocytes [103]. The p value 0.572>0.05, which is non-significant

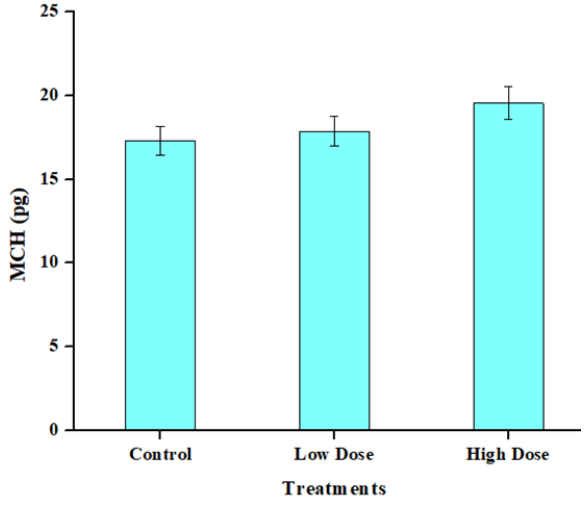

FIGURE 4.18: MCH (pg) level of all groups, when p value was <0.05

When compared with control group the MCH in low dose showed slightly less extension suggesting smaller red blood cells with less amount of hemoglobin per cell while MCH showed more extension in high dose group suggesting larger red blood cells with high amount of hemoglobin per cell.

4.4.7 MCHC

The Mean Corpuscular Hemoglobin Concentration (MCHC) is an important component of a complete blood count, gives valuable information about the average concentration of hemoglobin in the red blood cell [104]. MCHC reflects the ratio of hemoglobin concentration to the volume of individual erythrocytes. When compared to control group there was a little rise in MCHC values in the low dosage group and higher MCHC values in high dose group. The p value 0.475>0.05, which is non-significant.

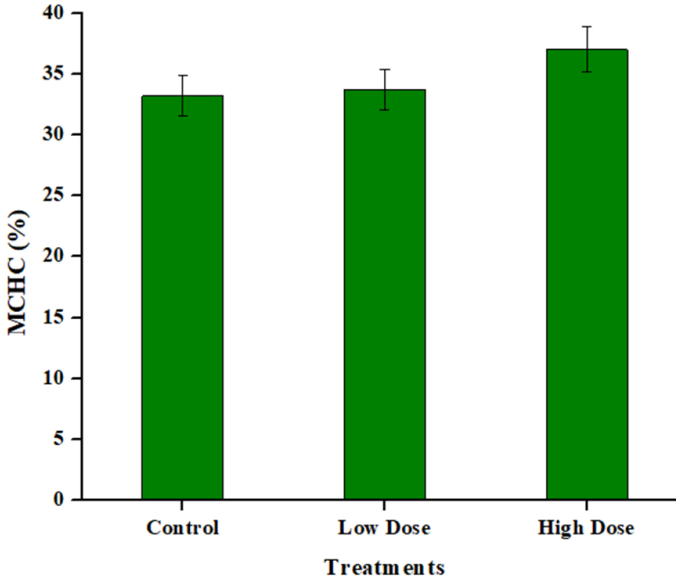

FIGURE 4.19: MCHC (g/dL) level of all groups, when p value was <0.05

4.4.8 Platelets Count

Platelets are vital components of the blood playing role in preventing and stops bleeding. Platelets are influential in maintaining the integrity of the circulatory

system [105]. When blood vessels are injured, platelets quickly respond in forming a blood clot. Thus, preventing excessive bleeding.

When compared to control group the platelets count of low dose group was exceeded which can form a clots of blood in the blood vessels, it also connected with infection or some kind of tumor development while there is also an increase platelets count in high dose group. The p value 0.334>0.05, which is non-significant.

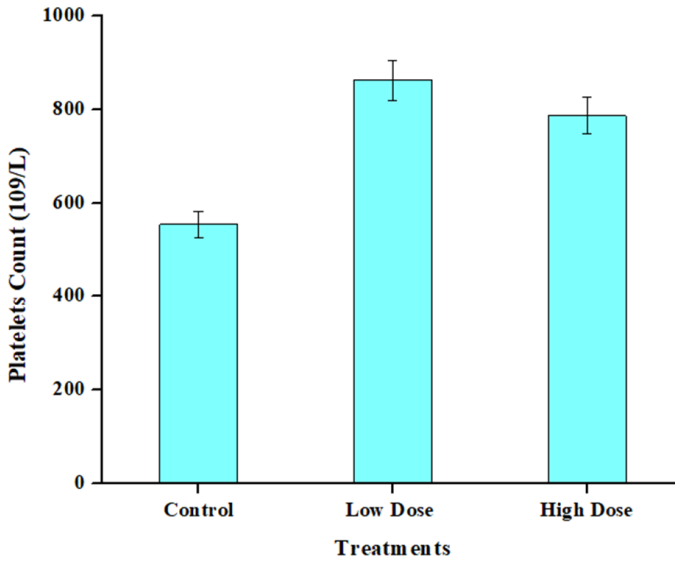

FIGURE 4.20: Platelets count (1000/mm^3) of all groups, when p value was <0.05

As demonstrated in the table four different parameters of hematology of the ZNS NPs dose taking groups were compared with control group in which MCV value of control, low and high dose group are 50.60±0.50, 53±3.29 and 52.46±2.19 respectively which means MCV value just slightly show increase in both low and high dose group. The MCH value of control, low and high dose group were 17.30±0.261, 17.86±1.07 and 19.53±4.30 respectively. This result demonstrates that MCH value is less in low and high dosage group rats as compared to control group.

The MCHC value of control, low and high dosage group rats were33.23±1.77, 33.76±0.20 and 37.03±6.47 respectively. When compared to control group there was a little rise in MCHC values in the low dosage group and higher MCHC values in high dose group. However the platelets count of three experimental groups were

554.33±135.65, 862.33±197.56 and 786.44±342.81 which shows that high dose of ZnS NPs have more causing effect on platelets count.

TABLE 4.6: MCV, MCH, MCHC and Platelets Count in three experimental groups in one way ANOVA with Mean±SD when p<0.05

Groups(n=3)	**MCV**	**MCH**	**MCHC**	**Platelet Count**
Control	50.60 ± 0.50	17.30 ± 0.26	33.23 ± 1.77	554.33 ± 135.65
Low Dose	53 ± 3.29	17.86 ± 1.07	33.76 ± 0.20	862.33 ± 197.56
High Dose	52.46 ± 2.19	19.53 ± 4.30	37.03 ± 6.47	786.44 ± 342.81

4.4.9 Neutrophils

Neutrophils are a crucial component of the immune system, functions as frontline defenders against bacterial, pathogenic and fungal infections. These white blood cells are part of the innate immune response and provide rapid and immediate protection on encountering pathogens [106].

There are low levels of neutrophils in both low dose and high dose groups when compared to control group indicating that body has a difficulty in fighting of infections making them more prone to serious illnesses. The p value 0.012<0.05, which is statistically significant

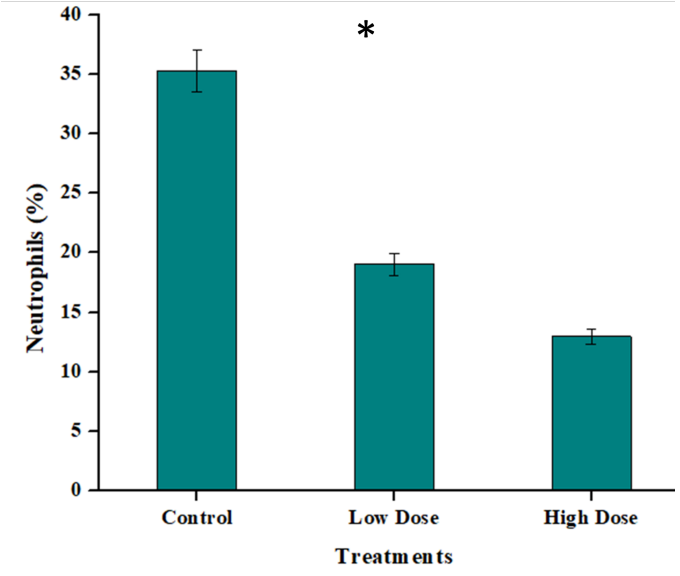

FIGURE 4.21: Neutrophils level (%) of all groups, when p value was <0.05

4.4.10 Lymphocytes

White blood cells are known as lymphocytes. They are a significant part of the immune system. They provide protection to the body against viruses, infections, and other harmful foreign substances [107].

There was a slight decrease in lymphocytes count in low dose group, considering unnoticeable as compared to other groups. The p value 0.950>0.05, which is non-significant

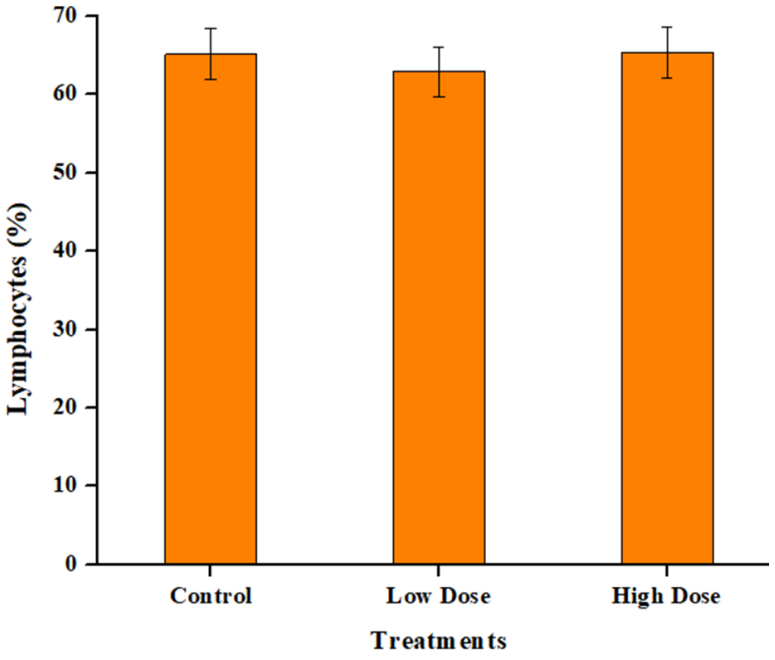

FIGURE 4.22: Lymphocytes level (%) of all groups, when p value was <0.05

4.4.11 Monocytes

Monocytes are white blood cell type provide important role in maintaining integrity to the immune system's function. Their primary role is to provide immediate and nonspecific defense against a variety of pathogens including bacterial and viral infections.

The monocytes rate of dosage groups (low and high) were decreases gradually as compared to control group. High monocytes level can be caused by any stress or recovery from an infection. The p value 0.295>0.05, which is non-significant.

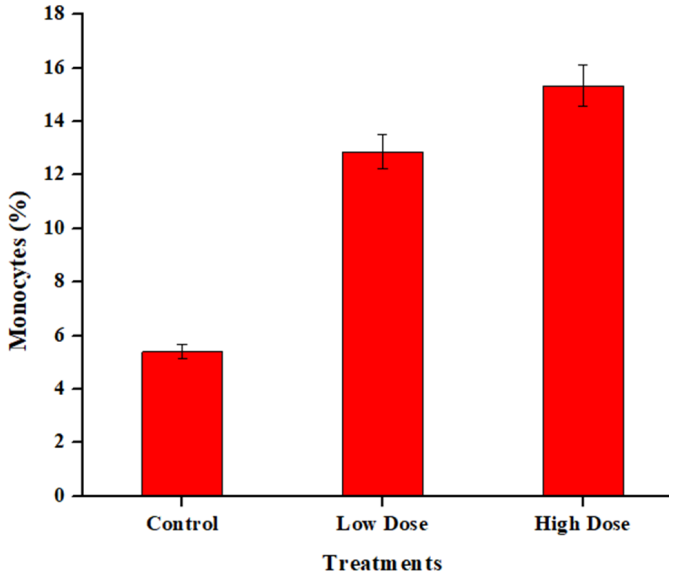

FIGURE 4.23: Monocytes level (%) of all groups, when p value was <0.05

4.4.12 Eosinophils

Eosinophils are a type of white blood cell and play a crucial role in the immune system. The results shows that there were significantly low eosinophils count observed in low dose group and slightly decrease also observe in high dose group as compared to control one. The p value 0.560>0.05, which shows the results are non-significant.

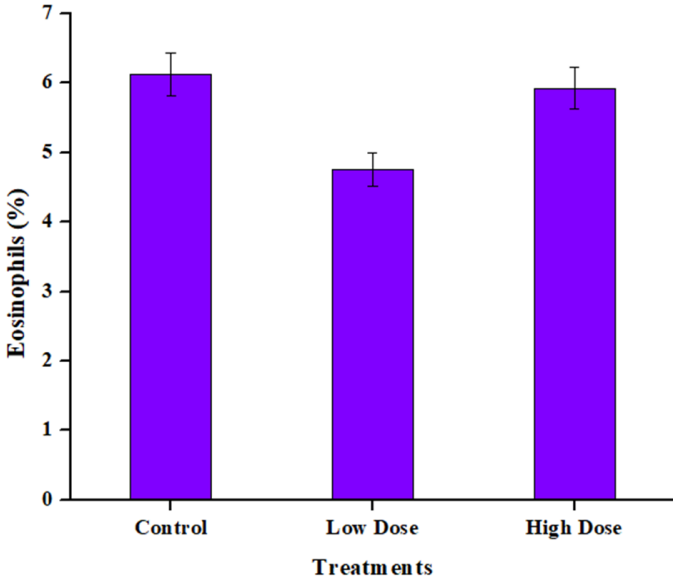

FIGURE 4.24: Eosinophils level (%) of all groups, when p value was <0.05

The four parameters of leukocyte count of dosage groups were compared with control group in which neutrophils count of control, low and high dose group were 35.33±3.80, 19.03±6.12 and 12.96±8.18. There are low levels of neutrophils in both low dose and high dose groups when compared to control group. The lymphocytes count of control, low and high dose group were 33.33±3.51, 62.96±7.91 and 65.40±15.50 respectively which means there was a slight decrease in lymphocytes count in low dose group, considering unnoticeable as compared to other groups.

The Monocytes count of the three experimental groupswere 5.40±0.43, 12.86±4.56 and 15.33±11.87 respectively. The monocytes results was slightly high in low dose group. The monocytes rate of low dose and high dose group were decreases gradually as compared to control group. Eosinophil of control, low and high dose group were 6.13±1.42, 4.76±0.90 and 5.93±2.19 respectively. The results shows that there were significantly low Eosinophils count observed in low dose group and slightly decrease also observe in high dose group as compared to control one.

TABLE 4.7: Neutrophils, lymphocytes, monocytes and eosinophils of dosage groups compared with control group in one way ANOVA with Mean±SD when $p<0.05$

Groups (n=3)	**Neutrophils**	**Lymphocytes**	**Monocytes**	**Eosinophils**
Control	35.33 ± 3.80	33.33 ± 3.51	5.40 ± 0.43	6.13 ± 1.42
Low Dose	19.03 ± 6.12	62.96 ± 7.91	12.86 ± 4.56	4.76 ± 0.90
High Dose	12.96 ± 8.18	65.40 ± 15.50	15.33 ± 11.87	5.93 ± 2.19

4.5 Liver Function Test (LFT)

4.5.1 Protein Total

Total protein measures the amount of protein in blood for Liver Function Tests (LFTs), which are a group of blood tests used to measure the health and functionality of the liver. It gives valuable information regarding the liver's synthetic function and overall protein metabolism [108].

The protein total of all the rats in high dose group is similar to the control group but in low dose taking group of ZnS NPs a slight increase in amount was observed. The p value 0.661>0.05, which is non-significant.

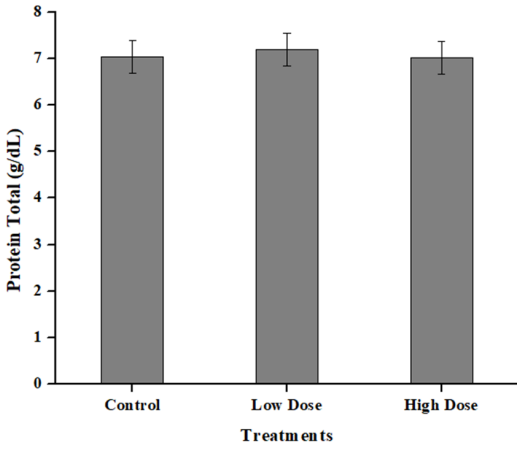

FIGURE 4.25: Protein Total (g/dL) level of all groups, when p value was <0.05

4.5.2 Alanine Transaminase

ALT is an important marker for assessing the liver health. It is found within liver cells (hepatocytes). The blood levels of this enzyme increase in response to any inflammation or injury to the liver, which releases ALT into the circulation [109].

After biochemical analysis the ALT level both in low and high dose group vigorously increaseed which means after intake of Green-synthesized ZnS nanoparticles liver cells are damage. The p value 0.000<0.001, which shows the results are extremely significant.

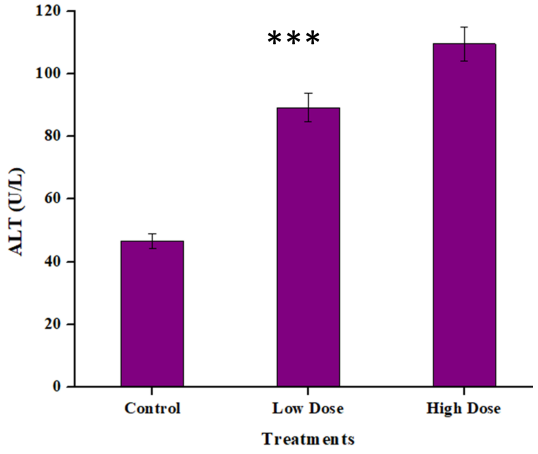

FIGURE 4.26: ALT level (U/L) of all groups, when p value was <0.05

4.5.3 Total Bilirubin

Total bilirubin is produced during the breakdown of red blood cells and plays an important role in liver and gallbladder function.

After biochemical analysis of blood it was observed that there was vigorously increase in bilirubin in high dose group but slight increase was also observed in low dose group when compared with control group. High bilirubin leads to Jaundice and can leak out in the pee and making it darker. The p value 0.005<0.01, which is very significant.

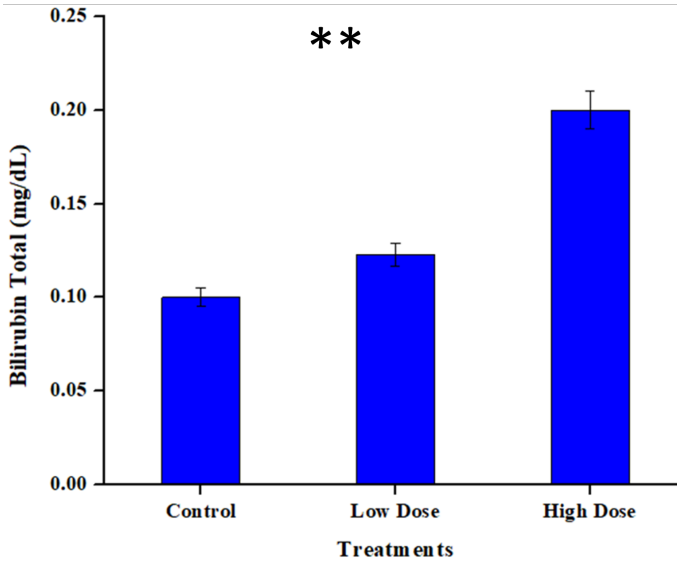

FIGURE 4.27: Total bilirubin level (mg/dL) of all groups, when p value was <0.05

4.5.4 Alkaline Phosphatase

Alkaline phosphatase measures the amount of enzyme ALP in liver, bones, kidneys, and intestines. The liver is a major source of alkaline phosphatase in the blood [110].

Higher levels of ALP can be an indicator of liver diseases and in this case there was gradually increase in ALP in high dose group and slightly low increase in low dose group when compared to control group [111]. The p value 0.067>0.05, which is non-significant.

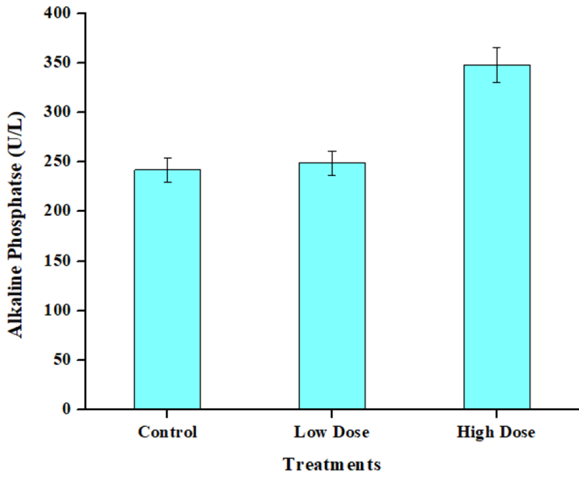

FIGURE 4.28: Alkaline phosphatase level (U/L) of all groups, when p value was <0.05

4.5.5 Aspartate aminotransferase (AST)

AST measures the amount of an enzyme that is found in liver cells and measured in liver function test (LFT). AST has a primary role in breaking down of amino acid by liver cells and converting food into energy.

High AST levels can be an indicator of damaged liver cells and leaks out of liver into bloodstream. In this case there is an increase in AST level in both low and high dose groups, when compared to control group. The p value 0.000<0.001, which is extremely significant.

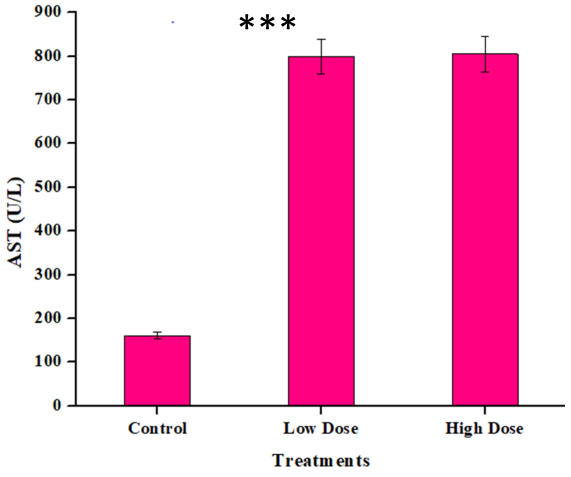

FIGURE 4.29: Aspartate aminotransferase Level (U/L) of all groups, when p value was <0.05

4.5.6 Albumin

It is a crucial protein in blood and is a part of Liver Function Test. It also has an important role in carrying important hormones and enzymes throughout the body.

An increase in Albumin level was observed in both low and high dose groups which is often a sign of dehydration, when compared to control group. The p value 0.051>0.05, which is non-significant.

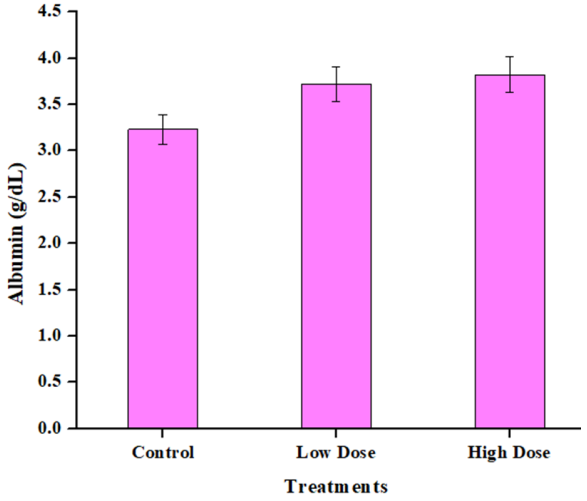

FIGURE 4.30: Albumin Level (g/dL) for all groups, when p value was <0.05

4.5.7 Globulins

Globulins are the proteins in the blood produced by the liver and immune system. They provide information regarding liver and kidney function [112].

In this study there is a gradual increase in Globulins level in low dosage group may indicating any infection or inflammation while decrease level in high dose taking group of ZnS NPs may indicating liver disease or malnutrition, when compared to control group. The p value 0.174>0.05 which is non-significant.

The LFT parameters of dosage groups are compared with control group. The protein total levels of the three experimental groups were 7.05±0.07, 7.20±0.20 and 7.03±0.37 respectively which means all the values are approximately same,

but there a slight increase in amount was observed in low dose group. The ALT level of the experimental groups were 46.66±2.51, 89.33±12.05 and 109.66±10.59 respectively. ALT level both in low and high dosage group rats vigorously increased after intake of Green-synthesized ZnS nanoparticles and it indicates a liver damage. The total bilirubin of control, low and high dose group were 0.10±0, 0.12±0.40 and 0.20±0 consecutively. It was observed that there was vigorously increase in bilirubin in high dose group but slight increase was also observed in low dose group. Alkaline phosphate was gradually increase in high dose group and slightly low increase in low dose group when compared to control group and the values of alkaline phosphate of the experimental groups were 242.33±10.69, 249±59.22 and 348.33±60.05.

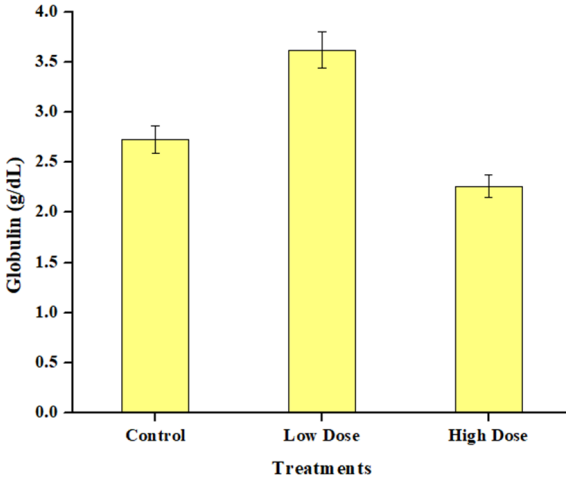

FIGURE 4.31: Globulins Level (g/dL) for all groups, when p value was <0.05

TABLE 4.8: Protein Total, ALT, Total Bilirubin and Alkaline Phosphatase levels in control, low dose and high dose group in one way ANOVA along with Mean±SD when p <0.05

Groups (n=3)	**ALT(SGPT)**	**Protein Total**	**Total Bilirubin**	**Alkaline Phosphatase**
Control	46.66 ± 2.51	7.05 ± 0.07	0.10 ± 0	242.33 ± 10.69
Low Dose	89.33 ± 12.05	7.20 ± 0.20	0.12 ± 0.40	249 ± 59.22
High Dose	109.66 ± 10.59	7.03 ± 0.37	0.20 ± 0	348.33 ± 60.05

The AST of the three experimental groups were 160.66±11.06, 799.33±118.96 and 804.33±136 consecutively. There is an increase in AST level in both low and high dose groups, when compared to control group. Albumin of control, low and high

dose group were 3.23±0.11, 3.72±0.05 and 3.82±0.39 respectively. An increase in Albumin level was observed in both low and high dose groups which is often a sign of dehydration, when compared to control group. Globulins level of three experimental groups were 3.82±0.39, 3.82±0.39 and 2.26±1.32 respectively.

In this study there is a gradual increase in Globulins level in low dosage group may indicating any infection or inflammation while there is a decrease in the level in high dose group indicating liver disease or malnutrition, when compared to control group

TABLE 4.9: AST, Albumin and Globulins levels in control, low dose and high dose group in one way ANOVA along with Mean±SD when p <0.05

Groups (n=3)	**AST**	**Albumin**	**Globulins**
Control	160.66 ± 11.06	3.23 ± 0.11	3.82 ± 0.39
Low Dose	799.33 ± 118.96	3.72 ± 0.05	3.82 ± 0.39
High Dose	804.33 ± 136	3.82 ± 0.39	2.26 ± 1.32

4.6 Renal Function Test (RFT)

4.6.1 Urea

Urea is a principle component measured in Renal Function Tests (RFTs), which are blood tests provide information about the health and function of the kidneys [113].

After analysis high urea rate were observed in case of low and high dose group, when compared to control group. It is a sign of kidney disease or injury. The p value 0.119>0.05 which is non-significant.

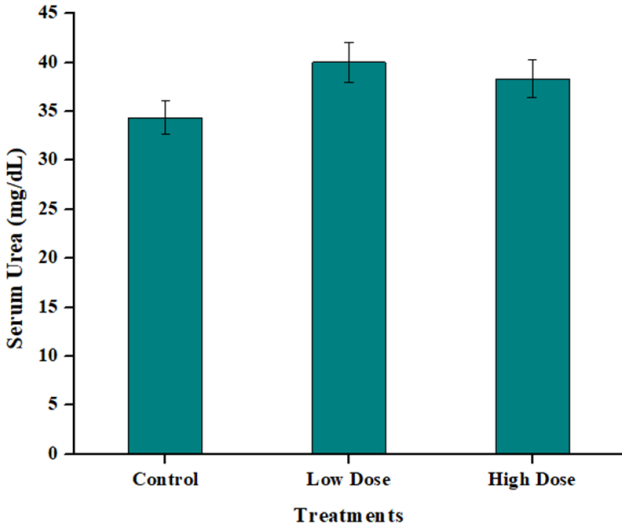

FIGURE 4.32: Urea level (mg/dL) of all groups, when p value was <0.05

4.6.2 Creatinine

Creatinine is a key parameter measured in Renal Function Tests (RFTs). It is the produced by muscles as waste product which filters out of the kidney. It plays a significant role in assessing the health and function of the kidneys [114].

After biochemical analysis higher level of creatinine was observed in low dose group and slightly higher levels than control was observed in high dosage group, when compared to control group which was a sign of kidney damage or kidney infection. The p value 0.398>0.05 which is non-significant.

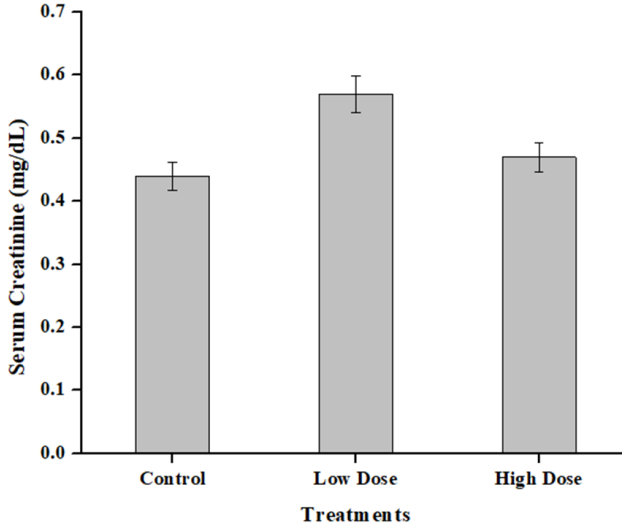

FIGURE 4.33: Creatinine level (mg/dL) of all groups, when p value was <0.05

4.6.3 Serum BUN

It is a waste product produced by the breakdown of proteins by liver. It measures the amount of urea nitrogen in blood and plays an essential role in Renal Function Tests (RFTs), where its levels in the blood are measured to assess kidney function. After biochemical analysis low level of blood urea nitrogen is observed in case of low dose and high dose group, when compared to control group. Low BUN levels indicates over-hydration or liver damage. The p value 0.028<0.05 which is statistically significant.

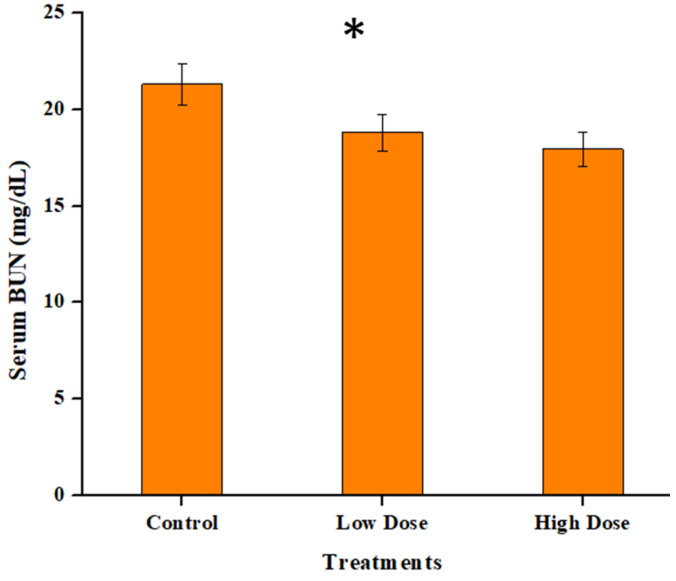

FIGURE 4.34: Serum BUN level (mg/dL) of all groups, when p value was <0.05

There was comparison between RFT of both low dose and high dose group with control wherein case of both low and high dose group, higher urea rate were observed when compared with control group. The control, low and high dose group urea values were 34.33±2.88, 40±3.46 and 38.33±2.08 respectively. The increasing levels of creatinine in low dosage groups rats was observed and marginally increased levels than control was found in higher dosage group, that was a sign of kidney damage or kidney infection and creatinine level of control low and high dose group were 0.44±0.13, 0.57±0.13 and 0.470.02 respectively. BUN level in three experimental groups were 21.33±0.11, 18.81±1.76 and 17.96±0.92 respectively. The low level of blood urea nitrogen is observed in case of low dose and

high dose group, when compared to control group. Low BUN levels indicates over hydration or liver damage.

If recorded p-value is <0.05, it indicates the significance of these results.

TABLE 4.10: Urea, creatine and serum BUN levels in control, low dose and high dose group creatinine in one way ANOVA along with Mean±SD when p<0.05,

Groups (n=3)	**Urea**	**Creatinine**	**Serum BUN**
Control	34.33 ± 2.88	0.44 ± 0.13	21.33 ± 0.11
Low Dose	40 ± 3.46	0.57 ± 0.13	18.81 ± 1.76
High Dose	38.33 ± 2.08	0.470.02	17.96 ± 0.92

4.7 Histopathology of Liver

4.7.1 Control Group

Microscopy: This Photomicrograph of rat liver tissue reveals intact architecture. There is no inflammation or malignancy in control group.There is no substantial inflammatory infiltration or necrosis observed in the field.

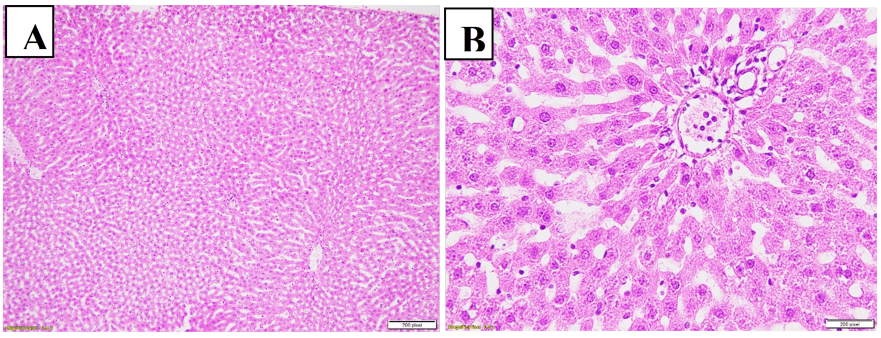

FIGURE 4.35: Liver histopathology with normal physiology

4.7.2 Low Dose Group

Microscopy: This Photomicrograph of rat liver tissues reveals mild cytoplasmic vacuolation within hepatocytes. The sinusoids appear mildly dilated, and Kupffer

cells are moderately prominent, suggesting mild activation and mild fatty degeneration or hydropic changes. The sinusoidal spaces are mildly dilated, and there is no significant inflammatory cell infiltration visible. These findings reveal a liver with mild metabolic stress, possibly due to early-stage toxic or nutritional disturbances.

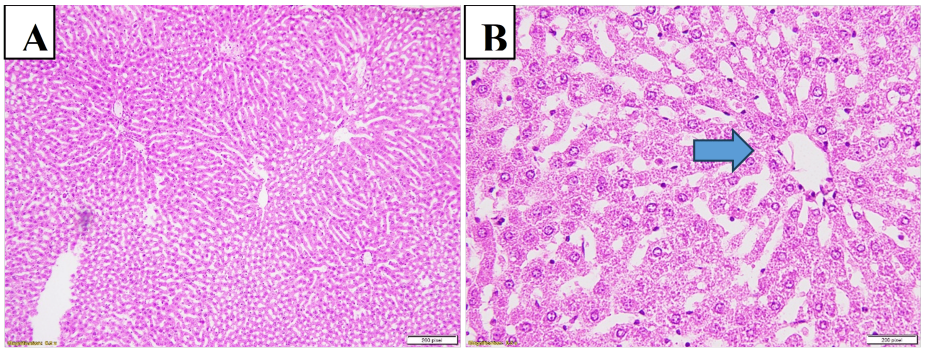

FIGURE 4.36: Liver Histopathology results with mild cytoplasmic vacuolation and fatty changes

4.7.3 High Dose Group

Microscopy: This Photomicrograph of Rat liver tissue reveals relatively preserved hepatic architecture with noticeable pathological features. Inflammatory cell infiltration (arrow) is observed around the portal areas, indicative of mild portal inflammation. Hepatocytes display prominent vacuolar degeneration, characterized by clear spaces within the cytoplasm, suggesting metabolic or toxic stress. The central vein appears intact, and sinusoidal spaces are mildly dilated, which may indicate early congestion. These changes are consistent with mild liver injury, with ongoing inflammation and hepatocellular degeneration.

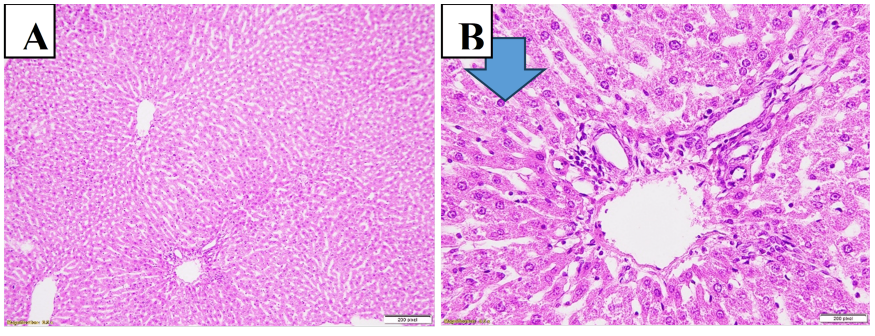

FIGURE 4.37: Liver histopathology with mild liver injury and mild portal inflammation

Chapter 5

Conclusion and Future Prospects

Zinc Sulfide Nanoparticles (ZnS NPs) are effective fluorescent markers for bioimaging because of their high photoluminescence. But these nanoparticles cause nanotoxicity through a number of pathways related to their specific physical and chemical properties. They can interact with numerous cellular components, causing oxidative stress and cytotoxicity. Reactive oxygen species (ROS) generated by the ZnS NPs results in oxidative stress that disrupts lipids, proteins, and DNA in cells with possibilities such as apoptosis or inflammation or genotoxicity.

Understanding nanotoxicity is essential to grasping long-term effects, especially for consumers purchasing products containing nanoparticles and workers in organizations using nanomaterials. To ensure safety, compliance, and the responsible development of nanotechnology, it is crucial to comprehend nanotoxicity. It is essential for safeguarding both the environment and human health while facilitating the development of novel materials and applications. In 2019, similar studies conducted in order to evaluate the cytotoxic properties of Green-synthesized ZnS nanoparticles against MCF-70 cancer cell line.

The main purpose of this research was to investigate the in-vivo toxicity of plant-extracted manufactured ZnS nanoparticles with the help of *Justicia adhatoda* extract. Green synthesis of ZnS NPs is an environment friendly method by using plant extracts that act as reducing and stabilizing agents. By understanding the in-vivo toxicity of the green synthesized ZnS NPs, it will help out for their safety

profile as well and may identify any biological damage. By understanding these above interactions between the nanoparticles mediated by plants and biological systems, we would be able to develop a protocol that leads to safety-assured application against human health and environment.

The synthesis of ZnS nanoparticles by using plant extract is an eco-friendly method, but it may still cause numerous disruptions inside the complex biological systems and leading to inflammation and genotoxicity. There are lack of knowledge on the cytotoxicity of Green synthesized ZnS NPs on an animal model. The research purpose is to evaluate a comprehensive In –vivo toxicity effects of Green –Synthesized ZnS NPs on an animal model.

The in-vivo toxicity and safety profile assessment was checked using morphological, biochemical, histopathological and hematological response of rats (*Justicia adhatoda*) after intake of Green-synthesized ZnS NPs. The results showed significant differences in different parameters like RBC Count, WBC Count, platelets, ALT, AST, Urea and creatinine level by making a comparison with control group through statistical analysis (one-way ANOVA). According to histopathological response low dose group shows mild cytoplasmic vacuolation within hepatocytes and mild metabolic stress, possibly due to early-stage toxic or nutritional disturbances while high dose group shows mild portal inflammation with prominent vacuolar degeneration in hepatocytes and these changes are consistent with mild liver injury. So, a comprehensive research and updated data is necessary to assess Green- synthesized ZnS NPs safety profile, particularly with regard to their biocompatibility in biological systems and long-term exposure. The nanoparticles has remarkable potential to revolutionize and bring innovation in various fields. But their toxicity is a major and significant concern regarding their safe applications. By understanding their effects on biological systems it would help for safe protocols to develop leading towards safe biomedical and environmental applications.

However, there are still challenges to address, including the need to optimize large-scale synthesis while ensuring sustainability, performing comprehensive toxicity

studies to evaluate long-term impacts on health and the environment, and enhancing stability for industrial applications. If these hurdles are overcome, ZnS NPs could see widespread use across various industries.

Bibliography

[1] M. Sajid and J. Płotka-Wasylka, "Nanoparticles: Synthesis, characteristics, and applications in analytical and other sciences," Microchem. J., vol. 154, no. 104623, p. 104623, 2020.

[2] J. Madhavi and V. Prasad, "ZnS and ZnS/CdS core-shell Nano particles: Synthesis, properties and Perspectives," Surf. Interfaces, vol. 21, no. 100757, p. 100757, 2020.

[3] R. Singh and R. R. Singh, Optical properties of ZnS quantum dots: applications in solar cells and biomedicine. 2022.

[4] M. M. H. Farahani et al., "Synthesis and antibacterial activity of silver doped zinc sulfide/chitosan bionanocomposites: A new frontier in biomedical applications," Int. J. Biol. Macromol., vol. 280, no. Pt 4, p. 135934, 2025.

[5] A. B. Alwany, G. M. Youssef, E. E. Saleh, O. M. Samir, M. A. Algradee, and A. Alnehia, "Structural, optical and radiation shielding properties of ZnS nanoparticles QDs," Optik (Stuttg.), vol. 260, no. 169124, p. 169124, 2022.

[6] E.-J. Park, U. Jeong, C. Yoon, and Y. Kim, "Comparison of distribution and toxicity of different types of zinc-based nanoparticles: Distribution and Toxicity of Different Types of Zinc-Based Nanoparticles," Environ. Toxicol., vol. 32, no. 4, pp. 1363–1374, 2017.

[7] V. G. Reshma, A. Sabareeswaran, K. S. Rajeev, and P. V. Mohanan, "In vitro and In vivo toxicity analysis of zinc selenium/zinc sulfide (ZnSe/ZnS) quantum dots," Food Chem. Toxicol., vol. 145, no. 111718, p. 111718, 2020.

[8] G. Alak, Aquatic Toxicology in Freshwater: The Multiple Biomarker Approach. Cham: Springer Nature Switzerland, 2025.s

[9] A. Jain, Nanomaterials for Sustainable Development: Opportunities and Future Perspectives. Singapore; Singapore: Springer Nature, 2023.

[10] P. Aarthye, M. SureshKumar, and S. Gnanam, "Biogenic synthesis of zinc sulphide nanoparticles using Allium sativum extract and evaluation of antimicrobial activity," Interactions, vol. 245, no. 1, 2025.

[11] C. Zhang et al., "Progress, challenges, and future of nanomedicine," Nano Today, vol. 35, no. 101008, p. 101008, 2020

[12] A. Abdolmaleki, A. Asadi, K. Gurushankar, T. Karimi Shayan, and F. Abedi Sarvestani, "Importance of nano medicine and new drug therapies for cancer," Adv. Pharm. Bull., vol. 11, no. 3, pp. 450–457, 2021.

[13] J. Gonzalez-Valdivieso, A. Girotti, J. Schneider, and F. J. Arias, "Advanced nanomedicine and cancer: Challenges and opportunities in clinical translation," Int. J. Pharm., vol. 599, no. 120438, p. 120438, 2021.

[14] L.-P. Wu, D. Wang, and Z. Li, "Grand challenges in nanomedicine," Mater. Sci. Eng. C Mater. Biol. Appl., vol. 106, no. 110302, p. 110302, 2020.

[15] Q. Wu, W.-S. Miao, Y.-D. Zhang, H.-J. Gao, and D. Hui, "Mechanical properties of nanomaterials: A review," Nanotechnol. Rev., vol. 9, no. 1, pp. 259–273, 2020.

[16] A. Tawfik, "Nanomaterials: Classification, properties, and environmental toxicities," Environmental Technology & Innovation, vol. 20, 2020.

[17] M. Zubair et al., "Application of nanotechnology for targeted drug delivery and nontoxicity," International Journal of General Practice Nursing, vol. 2, no. 2, pp. 57–67, 2025.

[18] L. Sun et al., "Smart nanoparticles for cancer therapy," Signal Transduct. Target. Ther., vol. 8, no. 1, p. 418, 2023.

[19] P. Christian, F. Von der Kammer, M. Baalousha, and T. Hofmann, "Nanoparticles: structure, properties, preparation and behaviour in environmental media," Ecotoxicology, vol. 17, no. 5, pp. 326–343, 2008.

[20] S. Hu, R. Zhao, Y. Shen, and B. Lyu, "Revolutionizing drug delivery: The power of stimulus-responsive nanoscale systems," Chem. Eng. J., vol. 496, no. 154265, p. 154265, 2025.

[21] N. Chausali, J. Saxena, and R. Prasad, "Nanotechnology as a sustainable approach for combating the environmental effects of climate change," J. Agric. Food Res., vol. 12, no. 100541, p. 100541, 2023.

[22] Q. Bai et al., "Speciation, distribution and environmental risk of dominant silver-containing nanoparticles in the Taihu Lake, China," Environ. Pollut., no. 125726, p. 125726, 2025.

[23] G. Magdy, E. Aboelkassim, S. M. Abd Elhaleem, and F. Belal, "A comprehensive review on silver nanoparticles: Synthesis approaches, characterization techniques, and recent pharmaceutical, environmental, and antimicrobial applications," Microchem. J., vol. 196, no. 109615, p. 109615, 2025.

[24] M. Noga, J. Milan, A. Frydrych, and K. Jurowski, "Toxicological aspects, safety assessment, and green toxicology of silver nanoparticles (AgNPs)-critical review: State of the art," Int. J. Mol. Sci., vol. 24, no. 6, 2023.

[25] J. Jeevanandam et al., "Green approaches for the synthesis of metal and metal oxide nanoparticles using microbial and plant extracts," Nanoscale, vol. 14, no. 7, pp. 2534–2571, 2022.

[26] A. Nkele and F. I. Chinecherem, "Diverse synthesis and characterization techniques of nanoparticles," IntechOpen, 2020.

[27] G. M. Nair, T. Sajini, and B. Mathew, "Advanced green approaches for metal and metal oxide nanoparticles synthesis and their environmental applications," Talanta Open, vol. 5, no. 100080, p. 100080, 2022.

[28] A. A. Yaqoob, K. Umar, and M. N. M. Ibrahim, "Silver nanoparticles: various methods of synthesis, size affecting factors and their potential applications–a review," Appl. Nanosci., vol. 10, no. 5, pp. 1369–1378, 2020.

[29] S. I. Tsekhmistrenko, V. S. Bityutskyy, O. S. Tsekhmistrenko, L. P. Horalskyi, N. O. Tymoshok, and M. Y. Spivak, "Bacterial synthesis of nanoparticles: A green approach," Biosyst. Divers., vol. 28, no. 1, pp. 9–17, 2020.

[30] A. Zielińska et al., "Nanotoxicology and nanosafety: Safety-by-Design and testing at a glance," Int. J. Environ. Res. Public Health, vol. 17, no. 13, p. 4657, 2020.

[31] O. Bondarenko et al., "Nanotoxicology and nanomedicine: The Yin and Yang of nano-bio interactions for the new decade," Nano Today, vol. 39, no. 101184, p. 101184, 2021.

[32] Y.-H. Wu, S.-Y. Ho, B.-J. Wang, and Y.-J. Wang, "The recent progress in Nanotoxicology and nanosafety from the Point of View of both toxicology and ecotoxicology," Int. J. Mol. Sci., vol. 21, no. 12, p. 4209, 2020.

[33] M. Correa, "Antimicrobial metal-based nanoparticles: A review on their synthesis, types and antimicrobial action," Beilstein journal of nanotechnology, vol. 11, pp. 1450–1469, 2020.

[34] Z. Luo and H. Du, "Prospect of different types of magnetic Nanoparticles in stem cell therapy," Stem Cell Rev Rep, vol. 16, no. 4, pp. 675–683, 2020.

[35] A. B. Sengul and E. Asmatulu, "Toxicity of metal and metal oxide nanoparticles: a review," Environ. Chem. Lett., vol. 18, no. 5, pp. 1659–1683, 2020.

[36] S. R. Karnati, P. Agbo, and L. Zhang, "Applications of silica nanoparticles in glass/carbon fiber-reinforced epoxy nanocomposite," Compos. Commun., vol. 17, pp. 32–41, 2020.

[37] M. Chowdhury, "Green synthesis of novel green ceramic-based nanoparticles prepared by sol-gel technique for diverse industrial application," Results in Surfaces and Interfaces, vol. 14, 2025.

[38] Y. Cui et al., "Role of nanoparticle materials as water-based lubricant additives for ceramics," Tribol. Int., vol. 142, no. 105978, p. 105978, 2020.

[39] D. Zhang, "RETRACTED: Green Synthesis of Metallic Nanoparticles and Their Potential Applications to Treat Cancer," Frontiers in chemistry, vol. 8, 2020.

[40] P. Dikshit et al., "Green synthesis of metallic nanoparticles: Applications and limitations," Catalysts, vol. 11, no. 8, p. 902, 2021.

[41] N. Hossain, "Advances and significances of nanoparticles in semiconductor applications-A review," Results in Engineering, vol. 19, 2023.

[42] Z. H. Mahmoud, O. D. Abdalstar, and N. Sabah, "Semiconductor metal oxide nanoparticles: A review for the potential of H2S gas sensor application," Earthline Journal of Chemical Sciences, pp. 199–208, 2020.

[43] M. Bader, Nanoparticles for biomedical applications. Elsevier, 2020.

[44] B. Begines et al., "Polymeric nanoparticles for drug delivery: Recent developments and future prospects," Nanomaterials (Basel), vol. 10, no. 7, p. 1403, 2020.

[45] K. C. de Castro, J. M. Costa, and M. G. N. Campos, "Drug-loaded polymeric nanoparticles: a review," Int. J. Polym. Mater., vol. 71, no. 1, pp. 1–13, 2022.

[46] A. Zielińska et al., "Polymeric nanoparticles: Production, characterization, toxicology and ecotoxicology," Molecules, vol. 25, no. 16, p. 3731, 2020.

[47] S. Indoria, V. Singh, and M.-F. Hsieh, "Recent advances in theranostic polymeric nanoparticles for cancer treatment: A review," Int. J. Pharm., vol. 582, no. 119314, p. 119314, 2020.

[48] H. Sei and T. Koide, "Recent advances in siRNA delivery mediated by lipid-based nanoparticles," Advanced drug delivery reviews, vol. 154, pp. 64–78, 2020.

[49] L. M. Ickenstein and P. Garidel, "Lipid-based nanoparticle formulations for small molecules and RNA drugs," Expert Opin. Drug Deliv., vol. 16, no. 11, pp. 1205–1226, 2019.

[50] S. Tudu, "Structural, morphological and optical characterization of green synthesized ZnS nanoparticles using Azadirachta Indica (Neem) leaf extract," International Journal of Nano Dimension, vol. 2, 2020.

[51] M. Abdul Rauf Khan, "ZnS nanoparticles prepared by Prunus persica leaf extract: Morphological, optical and electrical properties," International Journal of Modern Physics B, vol. 38, 2025.

[52] H. Q. Alijani, S. Pourseyedi, M. Torkzadeh Mahani, and M. Khatami, "Green synthesis of zinc sulfide (ZnS) nanoparticles using Stevia rebaudiana Bertoni and evaluation of its cytotoxic properties," J. Mol. Struct., vol. 1175, pp. 214–218, 2019.

[53] P. L. Reddy et al., "Dielectric properties of polyvinyl alcohol (PVA) nanocomposites filled with green synthesized zinc sulphide (ZnS) nanoparticles," J. Mater. Sci.: Mater. Electron., vol. 30, no. 5, pp. 4676–4687, 2019.

[54] T. Munir et al., "Investigation of antibacterial and anticancer activities of copper, aluminum and nickel doped zinc sulfide nanoparticles," Sci. Rep., vol. 14, no. 1, p. 19304, 2025.

[55] A. Surendran, R. Tintu, K. S. Das, V. J. A. Nair, and P. Varghese, "Biomedical and anticancer potential of green synthesized chalcogenide zinc sulfide nanoparticles using different plant extracts as the capping agent," Braz. J. Phys., vol. 54, no. 6, 2025.

[56] M. Mahajan et al., "Green synthesis of ZnO nanoparticles using Justicia adhatoda for photocatalytic degradation of malachite green and reduction of 4-nitrophenol," RSC Adv., vol. 15, no. 4, pp. 2958–2980, 2025.

[57] Isha, P. Kumar, and A. N. Singh, "An overview of Justicia adhatoda: A medicinal plant but native invader in India," Conservation, vol. 5, no. 1, p. 2, 2025.

[58] U. Jayaweera, "Ethnopharmacological uses, phytochemistry, pharmacological activities and toxicity of Justicia adhatoda L.: a review," Discover Plants, vol. 1, 2025.

[59] A. Yadav and R. A. Sharma, "ANTIBACTERIAL POTENTIAL OF DIFFERENT EXTRACTS OF VARIOUS PARTS OF JUSTICIA ADHATODA L," Journal of Phytological Research, vol. 37, no. 1, 2025.

[60] M. Khan, "Pharmacognostic Study and Antimicrobial Screening of Justicia adhatoda L. Using in Silico and in Vitro Strategies," The Sciencetech, vol. 5, pp. 146–164, 2025.

[61] A. Basit, "Anti-inflammatory and analgesic potential of leaf extract of Justicia adhatoda L.(Acanthaceae) in Carrageenan and Formalin-induced models by targeting oxidative stress," Biomedicine & Pharmacotherapy, vol. 153, 2022.

[62] M. Joshi, G. Bhadauriya, and C. Shrivastav, "IMPORTANCE OF ADHATODA VASICA NEES IN TRADITIONAL SYSTEM OF MEDICINES: A REVIEW."

[63] Samuel et al., "Leaf extract, phytochemical studies and preparation of herbal formulation justicia adhatoda lehya," Int J Pharm Chem, pp. 14–22, 2025.

[64] P. Khandelwal et al., "Exploring the pharmacological and chemical aspects of pyrrolo-quinazoline derivatives in Adhatoda vasica," Heliyon, vol. 10, no. 4, p. e25727, 2025.

[65] C. Hano and B. H. Abbasi, "Plant-based green synthesis of nanoparticles: Production, characterization and applications," Biomolecules, vol. 12, no. 1, p. 31, 2021.

[66] S. Sarma and V. R. Rao, "Emerging synthesis and characterization techniques for hybrid polymer nanocomposites," Nanotechnology, vol. 35, no. 1, 2023.

[67] M. Namakka, "A review of nanoparticle synthesis methods, classifications, applications, and characterization," Environmental Nanotechnology, Monitoring & Management, vol. 20,

[68] S. Sheshmani and M. Mardali, "Harnessing the synergistic potential of ZnS nanoparticle-interfacing chitosan for enhanced photocatalytic degradation in aqueous media and textile wastewater," J. Polym. Environ., vol. 32, no. 11, pp. 5783–5805, 2025.

[69] W. S. Mohamed, M. Ezzeldien, A. H. Alshammari, K. Alshammari, S. Alhassan, and N. M. A. Hadia, "Facile hydrothermal synthesis and characterization of novel Co-doped ZnS nanoparticles with superior physical properties," Opt. Mater. (Amst.), vol. 157, no. 116345, p. 11 [40]

[70] S. Sheshmani and M. Mardali, "Harnessing the synergistic potential of ZnS nanoparticle-interfacing chitosan for enhanced photocatalytic degradation in aqueous media and textile wastewater," J. Polym. Environ., vol. 32, no. 11, pp. 5783–5805, 2025.

[71] W. S. Mohamed, M. Ezzeldien, A. H. Alshammari, K. Alshammari, S. Alhassan, and N. M. A. Hadia, "Facile hydrothermal synthesis and characterization of novel Co-doped ZnS nanoparticles with superior physical properties," Opt. Mater. (Amst.), vol. 157, no. 116345, p. 116345, 2025. 6345, 2025. 2023.

[72] S. Lee et al., "Mastication stimuli regulate the heartbeat rate through rhythmic regulation by the hypothalamic-autonomic system; molecular and telemetric studies in weaning-stage rats," Front. Neurosci., vol. 17, p. 1260655, 2023.

[73] A. G. Ramadan, A. A. M. Yassein, E. A. Eissa, M. S. Mahmoud, and G. M. Hassan, "Biochemical and histopathological alterations induced by subchronic exposure to zinc oxide nanoparticle in male rats and assessment of its genotoxicicty," J.Umm Al-Qura Univ. Appll. Sci., vol. 8, no. 1–2, pp. 41–49, 2022.

[74] N. S. Malik, S. Riaz, and M. A. Khan, "Comprehensive assessment of in vivo toxicity and safety profile of PEGylated copper sulfide nanoparticles in a rat model (Sprague dawley)," Bionanoscience, vol. 15, no. 1, 2025.

[75] F. M. Abdelhamid, H. A. Mahgoub, and A. I. Ateya, "Ameliorative effect of curcumin against lead acetate-induced hemato-biochemical alterations, hepatotoxicity, and testicular oxidative damage in rats," Environ. Sci. Pollut. Res. Int., vol. 27, no. 10, pp. 10950–10965, 2020.

[76] H. G. Tohamy, O. S. El Okle, A. A. Goma, M. M. Abdel-Daim, and M. Shukry, "Hepatorenal protective effect of nano-curcumin against nano-copper oxide-mediated toxicity in rats: Behavioral performance, antioxidant, anti-inflammatory, apoptosis, and histopathology," Life Sci., vol. 292, no. 120296, p. 120296, 2022.

[77] M. A. Hashem, A. Z. M. Zidan, and S. A. El-Mandrawy, "Potential perfection effects of silver nanoparticles against cisplatin side effects in hepatocellular carcinoma induced in Sprague Dawley albino rats: Hematological, biochemical, histopathological, and immunohistochemical alterations," Slov. Vet. Zb., vol. 60, no. 25-Suppl, 2023.

[78] K. Shkal and M. El, "Ameliorating effect of zinc oxide nanoparticles against hematotoxicity induced by cyclophosphamide in male albino rats," Advances in Hematology and Oncology Research, vol. 3, no. 1, pp. 26–31, 2020.

[79] M. M. Abbas, A. H. Mahmoud, and H. A. Abdelmonem, "Modulatory effects of Zn oxide nanoparticles on cardiotoxicity and hematological changes in irradiated rats," International Journal of Radiation Research, vol. 20, no. 4, pp. 851–855, 2022.

[80] E. M. Jubeer, M. A. Manthrammel, P. A. Subha, M. Shkir, K. P. Biju, and S. A. AlFaify, "Defect engineering for enhanced optical and photocatalytic properties of ZnS nanoparticles synthesized by hydrothermal method," Sci. Rep., vol. 13, no. 1, p. 16820, 2023.

[81] I.-M. Duinea, A. Tăbăcaru, P. Chiriță, N. Cioateră, A.-M. Ceoromila, and G. Cârâc, "Fabrication of very fine ZnS nanoparticles through surface organo-modification," in Springer Proceedings in Materials, Cham: Springer Nature Switzerland, 2025, pp. 25–37.

[82] T. F. Khan, M. Muhyuddin, S. Irum, M. A. Ali, S. W. Husain, and M. A. Basit, "Comparing the antioxidant and hemolytic activity of wet-chemically synthesized ZnO, ZnS, and ZnO/ZnS nanocomposite," Inorg. Chem. Commun., no. 113902, p. 113902, 2025.

[83] R. N. Jeyad and L. K. Abbas, "Optical And Structural Characteristics Of Sn-doped ZnS Thin Films For Sensing H2 Gas," Journal of Optics, pp. 1–9, 2025.

[84] M. Sylwia and J. Cichy, "Application of Fourier Transform Infrared (FTIR) Spectroscopy in Characterization of Green Synthesized Nanoparticles," Molecules, vol. 30, 2025.

[85] H. R. Rajabi, F. Sajadiasl, H. Karimi, and Z. M. Alvand, "Green synthesis of zinc sulfide nanophotocatalysts using aqueous extract of Ficus Johannis plant for efficient photodegradation of some pollutants," J. Mater. Res. Technol., vol. 9, no. 6, pp. 15638–15647, 2020.

[86] A. Verma, P. Chaudhary, A. Singh, R. K. Tripathi, and B. C. Yadav, "ZnS nanosheets in a polyaniline matrix as metallopolymer nanohybrids for flexible and biofriendly photodetectors," ACS Appl. Nano Mater., vol. 5, no. 4, pp. 4860–4874, 2022.

[87] S. Kannan, N. P. Subiramaniyam, and M. Sathishkumar, "A novel green synthesis approach for improved photocatalytic activity and antibacterial properties of zinc sulfide nanoparticles using plant extract of Acalypha indica and Tridax procumbens," J. Mater. Sci.: Mater. Electron., vol. 31, no. 12, pp. 9846–9859, 2020.

[88] A. Paul and N. A. G. Maria, "Phytochemical fingerprinting and evaluation of in silico anti-thrombotic properties of Justicia adhatoda L. and Cordia dichotoma Frost," Notulae Scientia Biologicae, vol. 15, pp. 11625–11625, 2023.

[89] R. Nagalakshmi and S. P. Anand, "Phytochemical Screening, Functional Group Identification and Evaluation of In vitro Antioxidant Activity of Ethanol Extracts of the Medicinal Shrub-Justicia adhatoda L," Journal of Stress Physiology & Biochemistry, vol. 20, pp. 167–174, 2025.

[90] S. Singh and A. K. Pratap, Unveiling the Therapeutic Potential: Isolation and Analgesic Activity of Justicia adhatoda Vasica (JAV).

[91] C. Narasimhaji, "Justicia adhatoda L. vasicin and vasicinone as bioactive phytochemical compounds: Isolation, characterization, and computational studies," Results in Chemistry, vol. 6, 2023.

[92] N. I. Sattigeri et al., "Synthesis, structural characterization, and photocatalytic application of ZnS quantum dots," Part. Part. Syst. Charact., 2025.

[93] K. K. Ilavenil, V. Senthilkumar, A. Kasthuri, and S. Sivaraman, "Nanoparticles (MgO) utilising Justicia adhatoda and an evaluation of their antimicrobial properties," Mater. Today, 2025.

[94] I. M. Mehedi, A. I. M. Iskanderani, M. S. Islam, H. Shah, V. Shrotriya, and M. B. Zaman, "Rapid one pot syntheses of magnetic Zn1-xFexS nanostructures: Enhancing properties of ZnS material for effective photocatalytic application," Ceram. Int., vol. 50, no. 9, pp. 16131–16141, 2025.

[95] H. Labiadh, "Synthesis of ZnS nanoparticles and the investigation of their structural, optical and electrical properties," Euro-Mediterranean Journal for Environmental Integration, pp. 1–12, 2025.

[96] M. Hambi et al., "Structural evolution and photocatalytic performance of ZnS–ZnO thin films synthesized by spray pyrolysis," Ceram. Int., vol. 50, no. 19, pp. 35902–35914, 2025.

[97] A. E. Samir, "Zinc nanoparticles ameliorated obesity-induced cardiovascular disease: role of metabolic syndrome and iron overload," Scientific reports, vol. 13, 2023.

[98] S. Kausar, F. Jabeen, M. A. Latif, and M. Asad, "Characterization, dose dependent assessment of hepatorenal oxidative stress, hematological parameters and histopathological divulging of the hepatic damages induced by Zinc oxide nanoparticles (ZnO-NPs) in adult male Sprague Dawley rats," Saudi J. Biol. Sci., vol. 30, no. 9, p. 103745, 2023.

[99] N. Rehman et al., "Exposure to zinc oxide nanoparticles induced reproductive toxicities in male Sprague Dawley rats," J. Trace Elem. Med. Biol., vol. 83, no. 127411, p. 127411, 2025.

[100] H. Kareem, "Evaluating the Hematological Impact of Zinc Oxide Nanoparticles in NMRI Mice: An in Vivo Study," energy, and environmental science, vol. 4.

[101] A. Susilo, "Evaluating the Hematological Impact of Zinc Oxide Nanoparticles in NMRI Mice: An in Vivo Study," Journal of Nanostructures, vol. 13, pp. 504–511, 2023.

[102] H. Ghafarifarsani et al., "Comparative effect of chemical and green zinc nanoparticles on the growth, hematology, serum biochemical, antioxidant parameters, and immunity in serum and mucus of goldfish, Carassius auratus (Linnaeus, 1758)," Biol. Trace Elem. Res., vol. 202, no. 3, pp. 1264–1278, 2025.

[103] D. G. Silva, "In vivo toxicity and genotoxicity of L-glutathione capped AgIn5Se8@ ZnS nanocrystals," Nano-Structures & Nano-Objects, vol. 38, 2025.

[104] A. Khan, "In-vivo anticoccidial efficacy of green synthesized iron-oxide nanoparticles using Ficus racemosa Linn leaf extract.(Moraceae) against Eimeria tenella infection in broiler chicks," Veterinary Parasitology, vol. 321, 2023.

[105] L. Li et al., "In vivo comparison of the biodistribution and toxicity of InP/ZnS quantum dots with different surface modifications," Int. J. Nanomedicine, vol. 15, pp. 1951–1965, 2020.

[106] K. Vdas, "Bioaccumulation of CdSe quantum dots show biochemical and oxidative damage in Wistar rats," Oxidative Medicine and Cellular Longevity, vol. 2023, 2023.

[107] B. Sial, "ZnO Nanoparticles Impact on Organ Systems in Rats: A Comprehensive Exploration of Diverse Exposure Pathways," Journal of Zoology and Systematics, pp. 37–51, 2023.

[108] A. Heba, "Biosynthesis of zinc oxide nanoparticles using bacillus paramycoides for in vitro biological activities and in vivo assessment against hepatorenal injury induced by CCl4 in rats," Applied Biochemistry and Biotechnology, pp. 1–21, 2025.

[109] F. Mirzaei et al., "Toxicity and hepatoprotective effects of ZnO nanoparticles on normal and high-fat diet-fed rat livers: Mechanism of action," Biol. Trace Elem. Res., vol. 203, no. 1, pp. 199–217, 2025.

[110] M. Mahjoubian, A. S. Naeemi, Z. Moradi-Shoeili, C. R. Tyler, and B. Mansouri, "Oxidative stress, genotoxic effects, and other damages caused by chronic exposure to silver nanoparticles (Ag NPs) and zinc oxide nanoparticles (ZnO NPs), and their mixtures in zebrafish (Danio rerio)," Toxicol. Appl. Pharmacol., vol. 472, p. 116569, 2023.

[111] J. Wu et al., "Spatiotemporal synergism in osteomyelitis treatment with photoactivated core-shell zinc oxide/silver sulfide heterogeneous nanoparticles," ACS Appl. Mater. Interfaces, vol. 16, no. 9, pp. 11194–11205, 2025. [81]

[112] L. Li et al., "In vivo comparison of the biodistribution and toxicity of InP/ZnS quantum dots with different surface modifications," Int. J. Nanomedicine, vol. 15, pp. 1951–1965, 2020.

[113] H. A. Abed, H. K. Kadhem, and D. Bayram, "Histopathological and biochemical study on the kidneys of male mice injected intraperitoneally with thioacetamide," Iraqi J. Sci., pp. 13–19, 2023.

[114] B. Sial, "ZnO Nanoparticles Impact on Organ Systems in Rats: A Comprehensive Exploration of Diverse Exposure Pathways," Journal of Zoology and Systematics, pp. 37–51, 2023.

[115] Moussaoui, M., & Saoudi Jean, R. (Eds.). (2010). Tunable optical properties of ZnS nanoparticles.